5. SCOUR

5.1. Steady uniform flow in open channels

This chapter is written with a view to bottom scour. The main outcome is the scour velocity as a function of the particle diameter. The coordinate system applied in this chapter is shown in Figure 34.
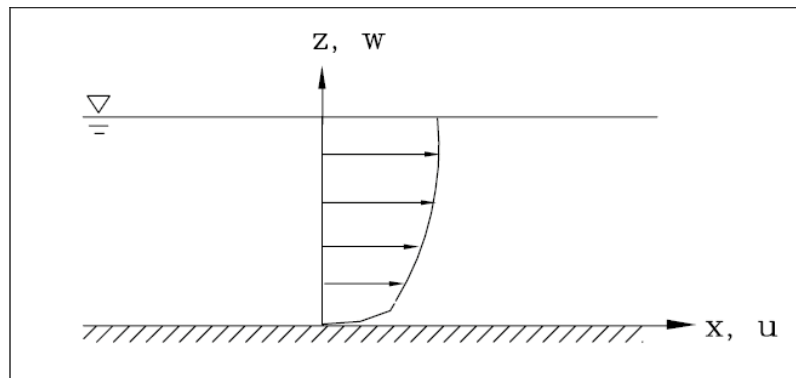
Figure 34: Coordinate system for the flow in open channels.

5.1.1. Types of flow

Description of various types of flow are given in the following.

Laminar versus turbulent

Laminar flow occurs at relatively low fluid velocity. The flow is visualized as layers which slide smoothly over each other without macroscopic mixing of fluid particles. The shear stress in laminar flow is given by Newton's law of viscosity:

$$\tau_v = \rho \cdot v \cdot \frac{du}{dz} \tag{5.1}$$

where ρ is density of water and v kinematic viscosity ($v = 10{-}6$ m^2/s at 200˚C). Most flows in nature are turbulent. Turbulence is generated by instability in the flow, which trigger vortices. However, a thin layer exists near the boundary where the fluid motion is still laminar. A typical phenomenon of turbulent flow is the fluctuation of velocity

$$U = u + u' \qquad W = w + w' \tag{5.2}$$

Where: U and W are instantaneous velocities, in x and z directions respectively
u and w time-averaged velocities, in x and z directions respectively
u' and w' instantaneous velocity fluctuations, in x and z directions respectively
Turbulent flow is often given as the mean flow, described by *u* and *w*. In turbulent flow the water particles move in very irregular paths, causing an exchange of momentum from one

portion of fluid to another, and hence, the turbulent shear stress (Reynolds stress). The turbulent shear stress, given by time-averaging of the Navier-Stokes equation, is:

$$\tau_t = -\rho \cdot \overline{u' \cdot w'} \tag{5.3}$$

Note that $\overline{u' \cdot w'}$ is always negative. In turbulent flow both viscosity and turbulence contribute to shear stress. The total shear stress is:

$$\tau = \tau_v + \tau_t = \rho \cdot \nu \cdot \frac{du}{dz} + \rho \cdot \overline{u' \cdot w'} \tag{5.4}$$

Steady versus unsteady

A flow is steady when the flow properties (e.g. density, velocity, pressure etc.) at any point are constant with respect to time. However, these properties may vary from point to point. In mathematical language:

$$\frac{\partial (any\_flow\_property)}{\partial t} = 0 \tag{5.5}$$

In the case of turbulent flow, steady flow means that the statistical parameters (mean and standard deviation) of the flow do not change with respect to time. If the flow is not steady, it is unsteady.

Uniform versus non-uniform

A flow is uniform when the flow velocity does not change along the flow direction, see Figure 35. Otherwise it is non-uniform flow.
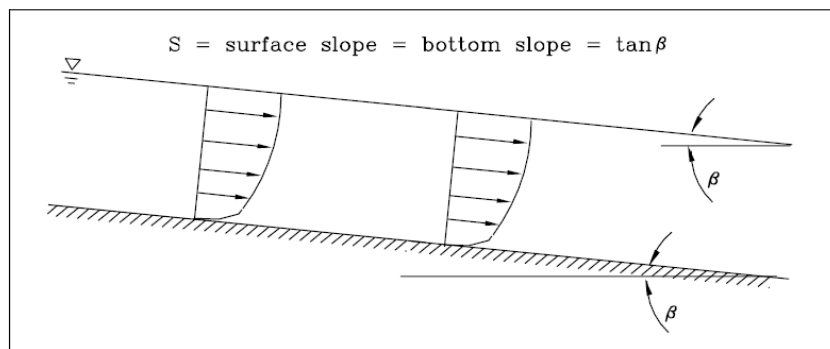
Figure 35: Steady uniform flow in a open channel.

Boundary layer flow

Prandtl developed the concept of the boundary layer. It provides an important link between ideal-fluid flow and real-fluid flow. Here is the original description.
For fluids having small viscosity, the effect of internal friction in the flow is appreciable only in a thin layer surrounding the flow boundaries.
However, we will demonstrate that the boundary layer fulfill the whole flow in open channels.

The boundary layer thickness $\boldsymbol{\delta}$ is defined as the distance from the boundary surface to the point where $\mathbf{u} = \mathbf{0.995 \cdot U}$. The boundary layer development can be expressed as:

Laminar flow $\qquad \dfrac{\boldsymbol{\delta}}{\mathbf{x}} = \mathbf{5} \cdot \left(\dfrac{\mathbf{U \cdot x}}{\boldsymbol{\nu}} \right)^{-0.5} \qquad$ when: $\qquad \mathbf{Re_x} = \dfrac{\mathbf{U \cdot x}}{\boldsymbol{\nu}} < \mathbf{5 \cdot 10^5} \qquad$ (5.6)

Turbulent flow $\qquad \dfrac{\boldsymbol{\delta}}{\mathbf{x}} = \mathbf{0.4} \cdot \left(\dfrac{\mathbf{U \cdot x}}{\boldsymbol{\nu}} \right)^{-0.2} \qquad$ when: $\qquad \mathbf{Re_x} = \dfrac{\mathbf{U \cdot x}}{\boldsymbol{\nu}} > \mathbf{5 \cdot 10^5} \qquad$ (5.7)
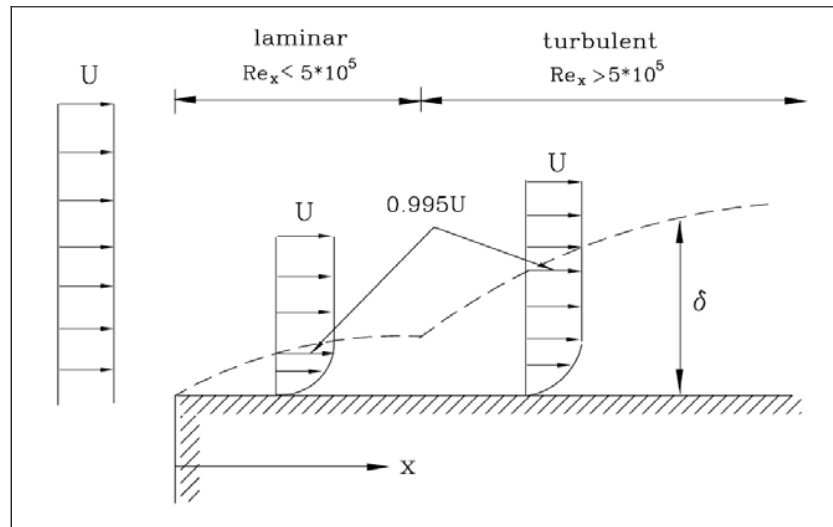
Figure 36: Development of the boundary layer.

5.1.2. Prandtl's mixing length theory

Prandtl introduced the mixing length concept in order to calculate the turbulent shear stress. He assumed that a fluid parcel travels over a length $\boldsymbol{\ell}$ before its momentum is transferred.
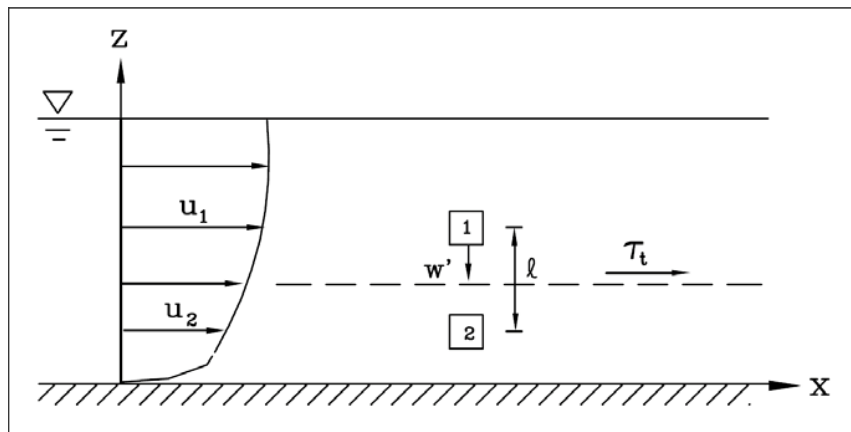
Figure 37: Prandtl's mixing length theory.

Figure 37 shows the time-averaged velocity profile. The fluid parcel, located in layer 1 and having the velocity $\mathbf{u_1}$, moves to layer 2 due to eddy motion. There is no momentum transfer during movement, i.e. the velocity of the fluid parcel is still $\mathbf{u_1}$ when it just arrives at layer 2,

and decreases to $\mathbf{u_2}$ some time later by the momentum exchange with other fluid in layer 2. This action will speed up the fluid in layer 2, which can be seen as a turbulent shear stress $\boldsymbol{\tau_t}$ acting on layer 2 trying to accelerate layer 2. The horizontal instantaneous velocity fluctuation of the fluid parcel in layer 2 is:

$$\mathbf{u'} = \mathbf{u_1} - \mathbf{u_2} = \ell \cdot \frac{\mathbf{du}}{\mathbf{dz}} \tag{5.8}$$

Assuming the vertical instantaneous velocity fluctuation having the same magnitude:

$$\mathbf{w'} = -\ell \cdot \frac{\mathbf{du}}{\mathbf{dz}} \tag{5.9}$$

where the negative sign is due to the downward movement of the fluid parcel, the turbulent shear stress now becomes:

$$\boldsymbol{\tau_t} = -\rho \cdot \mathbf{u'} \cdot \mathbf{w'} = \rho \cdot \ell^2 \cdot \left(\frac{\mathbf{du}}{\mathbf{dz}}\right)^2 \tag{5.10}$$

If we define kinematic eddy viscosity as:

$$\boldsymbol{\varepsilon} = \ell^2 \cdot \frac{\mathbf{du}}{\mathbf{dz}} \tag{5.11}$$

the turbulent shear stress can be expressed in a way similar to viscous shear stress:

$$\boldsymbol{\tau_t} = \rho \cdot \boldsymbol{\varepsilon} \cdot \frac{\mathbf{du}}{\mathbf{dz}} \tag{5.12}$$

5.1.3.   Fluid shear stress and friction velocity

Fluid shear stress

The forces on a fluid element with unit width is shown in Figure 38. Because the flow is uniform (no acceleration), the force equilibrium in x-direction reads:

$$\boldsymbol{\tau_z} \cdot \Delta \mathbf{x} = \rho \cdot \mathbf{g} \cdot (\mathbf{h} - \mathbf{z}) \cdot \Delta \mathbf{x} \cdot \sin(\beta) \tag{5.13}$$

For small slope we have $\sin(\beta) \approx \tan(\beta) = \mathbf{S}$. Therefore:

$$\boldsymbol{\tau_z} = \rho \cdot \mathbf{g} \cdot (\mathbf{h} - \mathbf{z}) \cdot \mathbf{S} \tag{5.14}$$

The bottom shear stress is:

$$\boldsymbol{\tau_b} = \boldsymbol{\tau_{z=0}} = \rho \cdot \mathbf{g} \cdot \mathbf{h} \cdot \mathbf{S} \tag{5.15}$$
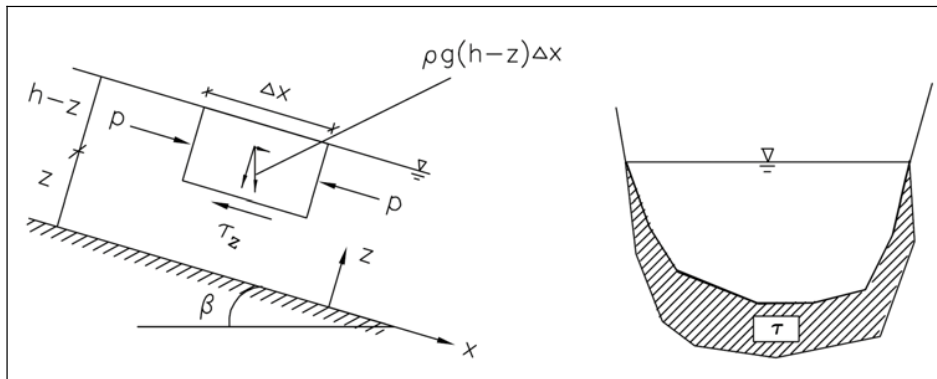
Figure 38: Fluid force and bottom shear stress.

Bottom shear stress

In the case of arbitrary cross section, the shear stress acting on the boundary changes along the wetted perimeter, cf. Fig.5. Then the bottom shear stress means actually the average of the shear stress along the wetted perimeter. The force equilibrium reads:

$$\tau_b \cdot O \cdot \Delta x = \rho \cdot g \cdot A \cdot \Delta x \cdot \sin(\beta) \qquad (5.16)$$

where **O** is the wetted perimeter and **A** the area of the cross section. By applying the hydraulic radius (**R = A/O**) we get:

$$\tau_b = \rho \cdot g \cdot R \cdot S \qquad (5.17)$$

In the case of wide and shallow channel, **R** is approximately equal to **h** and equation 5.15 is identical to equation 5.17.

Friction velocity

The bottom shear stress is often represented by friction velocity, defined by:

$$u_* = \sqrt{\frac{\tau_b}{\rho}} \qquad (5.18)$$

The term *friction velocity* comes from the fact that $\sqrt{\tau_b/\rho}$ has the same unit as velocity and it has something to do with friction force. Inserting equation 5.17 into equation 5.18, gives:

$$u_* = \sqrt{g \cdot R \cdot S} \qquad (5.19)$$

Viscous shear stress versus turbulent shear stress

Equation 5.15 states that the shear stress in flow increases linearly with water depth, see Figure 39.
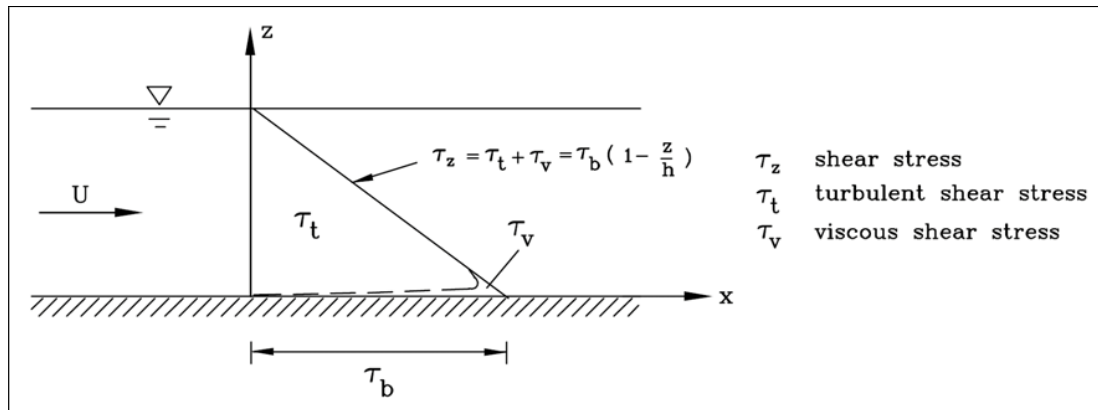
Figure 39: Shear stress components and distribution.

As the shear stress is consisted of viscosity and turbulence, we have:

$$\tau_z = \tau_v + \tau_t = \rho \cdot g \cdot (h - z) \cdot S \qquad (5.20)$$

On the bottom surface, there is no turbulence (**u=w=0, u'=w'=0**), the turbulent shear stress:

$$\tau_t = -\rho \cdot \overline{u' \cdot w'} = 0 \qquad (5.21)$$

Therefore, in a very thin layer above the bottom, viscous shear stress is dominant, and hence the flow is laminar. This thin layer is called viscous sub layer. Above the viscous sub layer, i.e. in the major part of flow, the turbulent shear stress dominates, see Figure 39. The measurement shows the shear stress in the viscous sub layer is constant and equal to the bottom shear stress, not increasing linearly with depth as indicated by Figure 39.

5.1.4. Classification of flow layers.

Scientific classification

Figure 40 shows the classification of flow layers. Starting from the bottom we have:
1. Viscous sub layer: a thin layer just above the bottom. In this layer there is almost no turbulence. Measurement shows that the viscous shear stress in this layer is constant. The flow is laminar. Above this layer the flow is turbulent.
2. Transition layer: also called buffer layer. viscosity and turbulence are equally important.
3. Turbulent logarithmic layer: viscous shear stress can be neglected in this layer. Based on measurement, it is assumed that the turbulent shear stress is constant and equal to bottom shear stress. It is in this layer where Prandtl introduced the mixing length concept and derived the logarithmic velocity profile.
4. Turbulent outer layer: velocities are almost constant because of the presence of large eddies which produce strong mixing of the flow.
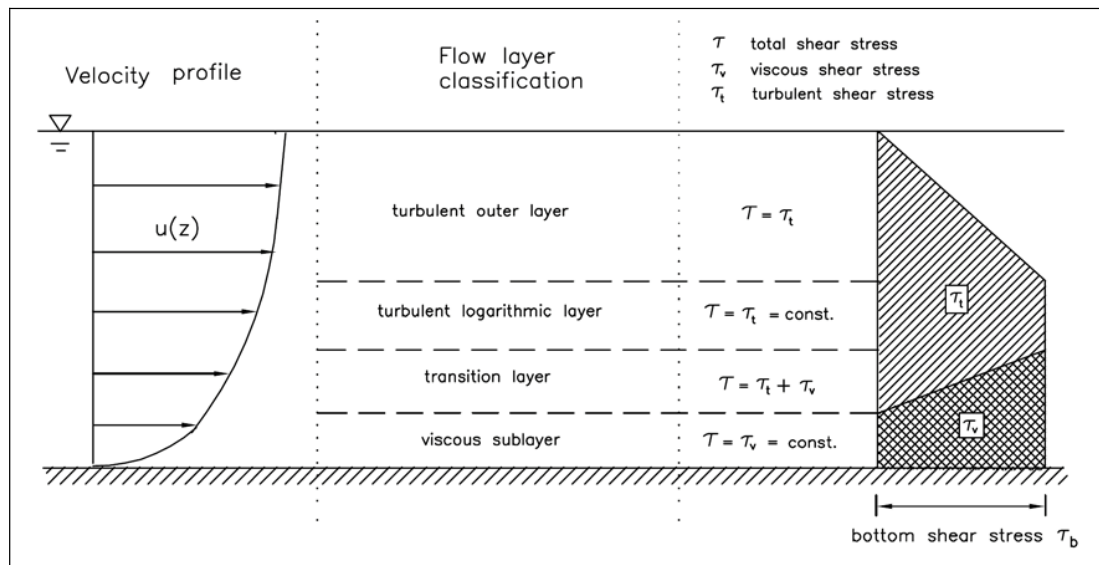
Figure 40: Scientific classification of flow region (Layer thickness is not to scale, turbulent outer layer accounts for 80% - 90% of the region).

Engineering classification

In the turbulent logarithmic layer the measurements show that the turbulent shear stress is constant and equal to the bottom shear stress. By assuming that the mixing length is proportional to the distance to the bottom ($\ell = \kappa z$), Prandtl obtained the logarithmic velocity profile.

Various expressions have been proposed for the velocity distribution in the transitional layer and the turbulent outer layer. None of them are widely accepted. However, by the modification of the mixing length assumption, see next section, the logarithmic velocity profile applies also to the transitional layer and the turbulent outer layer. Measurement and computed velocities show reasonable agreement.

Therefore in engineering point of view, a turbulent layer with the logarithmic velocity profile covers the transitional layer, the turbulent logarithmic layer and the turbulent outer layer, see Figure 41.

As to the viscous sub layer. The effect of the bottom (or wall) roughness on the velocity distribution was first investigated for pipe flow by Nikuradse. He introduced the concept of equivalent grain roughness $\mathbf{k_s}$ (Nikuradse roughness, bed roughness). Based on experimental data, it was found

1. Hydraulically smooth flow for $\dfrac{\mathbf{u_* \cdot k_s}}{\boldsymbol{\nu}} \leq \mathbf{5}$, Bed roughness is much smaller than the thickness of viscous sub layer. Therefore, the bed roughness will not affect the velocity distribution.

2. Hydraulically rough flow for $\dfrac{\mathbf{u_* \cdot k_s}}{\boldsymbol{\nu}} \geq \mathbf{70}$, Bed roughness is so large that it produces eddies close to the bottom. A viscous sub layer does not exist and the flow velocity is not dependent on viscosity.

3. Hydraulically transitional flow for $\mathbf{5} \leq \dfrac{\mathbf{u_* \cdot k_s}}{\boldsymbol{\nu}} \leq \mathbf{70}$, The velocity distribution is affected by bed roughness and viscosity.
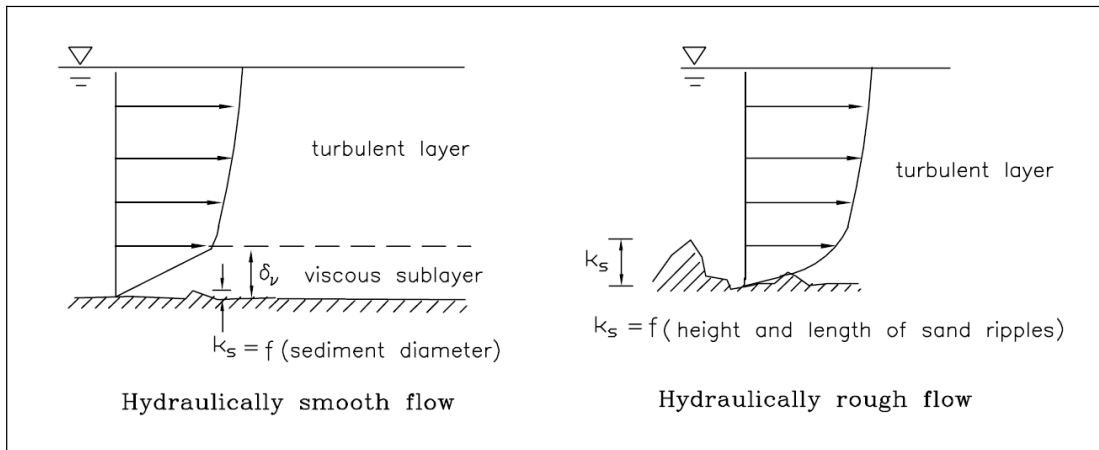
Figure 41: Engineering classification of flow region (Layer thickness is not to scale).

5.1.5. Velocity distribution

Turbulent layer

In the turbulent layer the total shear stress contains only the turbulent shear stress. The total shear stress increases linearly with depth (equation 5.15 or Figure 39), i.e.

$$\tau_t(z) = \tau_b \cdot \left(1 - \frac{z}{h} \right) \tag{5.22}$$

By Prandtl's mixing length theory:

$$\tau_t = \rho \cdot \ell^2 \left(\frac{du}{dz} \right)^2 \tag{5.23}$$

and assuming the mixing length:

$$\ell = \kappa \cdot z \cdot \left(1 - \frac{z}{h} \right)^{0.5} \tag{5.24}$$

with **κ** the Von Karman constant (**κ=0.4**) and **h>>z**, we get:

$$\frac{du}{dz} = \frac{1}{\kappa \cdot z} \cdot \sqrt{\frac{\tau_b}{\rho}} = \frac{u_*}{\kappa \cdot z} \tag{5.25}$$

Integration of the equation gives the famous logarithmic velocity profile:

$$u(z) = \frac{u_*}{\kappa} \cdot \ln \left(\frac{z}{z_0} \right) \tag{5.26}$$

where the integration constant z_0 is the elevation corresponding to zero velocity ($u_{z=z0}=0$), given by Nikuradse by the study of the pipe flows.

$$z_0 = 0.11 \cdot \frac{\nu}{u_*}$$ Hydraulically smooth flow $\frac{u_* \cdot k_s}{\nu} \le 5$ (5.27)

$$z_0 = 0.033 \cdot k_s$$ Hydraulically rough flow $\frac{u_* \cdot k_s}{\nu} \ge 70$ (5.28)

$$z_0 = 0.11 \cdot \frac{\nu}{u_*} + 0.033 \cdot k_s$$ Hydraulically transition flow $5 < \frac{u_* \cdot k_s}{\nu} < 70$ (5.29)

It is interesting to note that the friction velocity u_*, which, by definition, has nothing to do with velocity, is the flow velocity at the elevation $z=z_0 \cdot e^\kappa$, thus:

$$u_{z=z_0 \cdot e^\kappa} = u_*$$ (5.30)

In the study of sediment transport, it is important to know that the friction velocity is the fluid velocity very close to the bottom, see Figure 42.

Viscous sub layer

In the case of hydraulically smooth flow there is a viscous sub layer. Viscous shear stress is constant in this layer and equal to the bottom shear stress, i.e.

$$\tau_\nu = \rho \cdot \nu \cdot \frac{du}{dz} = \tau_b$$ (5.31)

Integrating and applying $u_{z=0}=0$ gives:

$$u(z) = \frac{\tau_b}{\rho} \cdot \frac{z}{\nu} = \frac{u_*^2}{\nu} \cdot z$$ (5.32)

Thus, there is a linear velocity distribution in the viscous sub layer. The linear velocity distribution intersect with the logarithmic velocity distribution at the elevation $z=11.6\nu/u_*$, yielding a theoretical viscous sub layer thickness:

$$\delta_\nu = 11.6 \cdot \frac{\nu}{u_*}$$ (5.33)

The velocity profile is illustrated in Figure 42, with the detailed description of the fluid velocity near the bottom.

Bed roughness

The bed roughness k_s is also called the equivalent Nikuradse grain roughness, because it was originally introduced by Nikuradse in his pipe flow experiments, where grains are glued to the smooth wall of the pipes. The only situation where we can directly obtain the bed roughness is a flat bed consisting of uniform spheres, where k_s = diameter of sphere.

OE4626 Dredging Processes

But in nature the bed is composed of grains with different size. Moreover, the bed is not flat, various bed forms, e.g. sand ripples or dunes, will appear depending on grain size and current. In that case the bed roughness can be obtained indirectly by the velocity measurement.
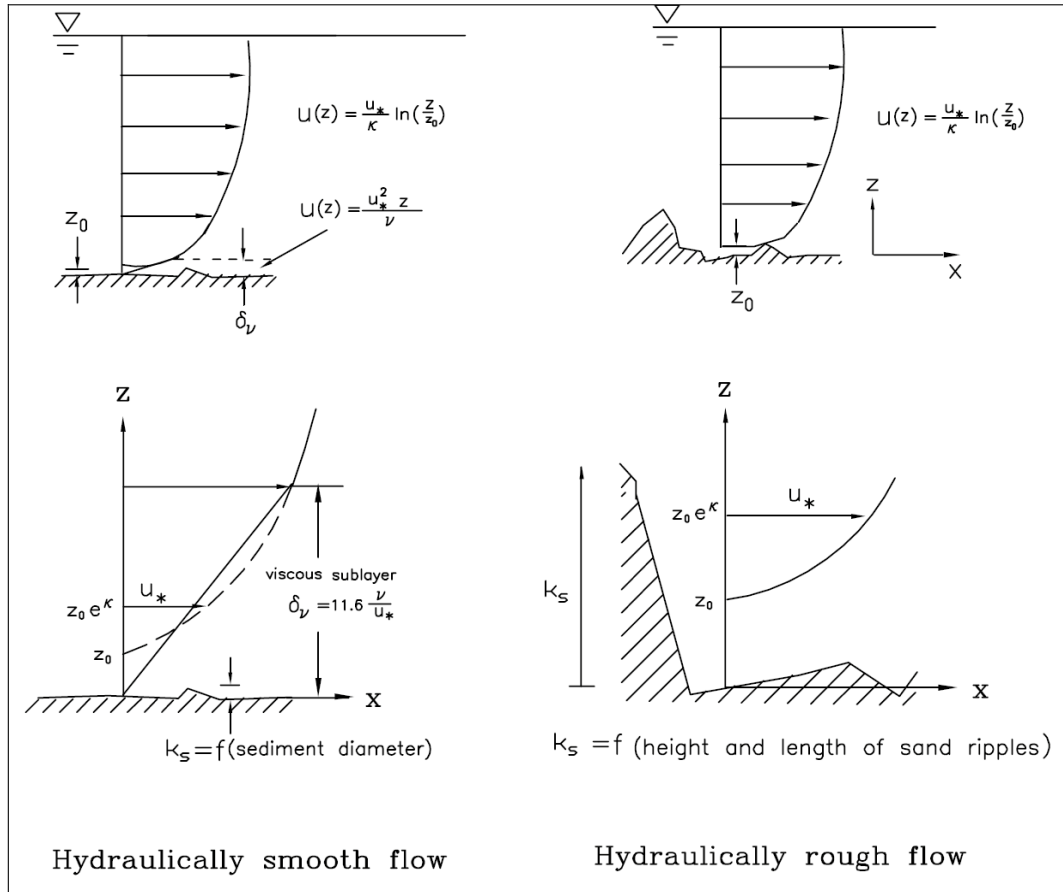
Figure 42: Illustration of the velocity profile in hydraulically smooth and rough flows.

5.1.6.   Chézy coefficient.

Chézy proposed an empirical formula for the average velocity of steady uniform channel flow:

$$U = C \cdot \sqrt{R \cdot S} \tag{5.34}$$

Where: R - Hydraulic radius, i.e. area of cross section divided by wetted perimeter
S - Bed slope
C - Empirical coefficient called Chézy coefficient. *C* was originally thought to be constant. Various formulas for *C* have been proposed.

Here we will see that **C** can be theoretically determined by averaging the logarithmic velocity profile. Recalling that the friction velocity is (equation 5.19) and applying it into equation 5.34, we get the expression of **C**:

$$C = \frac{U}{u_*} \cdot \sqrt{g} \tag{5.35}$$

Averaging the logarithmic velocity profile gives:

$$U = \frac{1}{h} \cdot \int_{z_0}^{h} u(z) \cdot dz = \frac{u_*}{\kappa \cdot h} \cdot \int_{z_0}^{h} \ln\left(\frac{z}{z_0}\right) \cdot dz \tag{5.36}$$

$$U = \frac{u_*}{\kappa} \cdot \left(\ln\left(\frac{h}{z_0}\right) - 1 + \frac{z_0}{h} \right) \approx \frac{u_*}{\kappa} \cdot \ln\left(\frac{h}{z_0 \cdot e}\right) \tag{5.37}$$

Inserting the above equation into equation 5.35 gives:

$$C = \frac{\sqrt{g}}{\kappa} \cdot \ln\left(\frac{h}{z_0 \cdot e}\right) = 2.3 \cdot \frac{\sqrt{g}}{\kappa} \cdot \log\left(\frac{h}{z_0 \cdot e}\right) \tag{5.38}$$

$$C = 2.3 \cdot \frac{\sqrt{g}}{\kappa} \cdot \log\left(\frac{h}{\left(0.11 \cdot \frac{\nu}{u_*} + 0.033 \cdot k_s \right) \cdot e} \right) = 18 \cdot \log\left(\frac{11.14 \cdot h}{3.33 \cdot \frac{\nu}{u_*} + k_s} \right) \tag{5.39}$$

This can be approximated by:

$$C \approx 18 \cdot \log\left(\frac{12 \cdot h \cdot u_*}{3.3 \cdot \nu}\right) \qquad \text{Hydraulically smooth flow} \qquad \frac{u_* \cdot k_s}{\nu} \le 5 \tag{5.40}$$

$$C \approx 18 \cdot \log\left(\frac{12 \cdot h}{k_s}\right) \qquad \text{Hydraulically rough flow} \qquad \frac{u_* \cdot k_s}{\nu} \ge 70 \tag{5.41}$$

where the expression for z_0 has been used and **ln** has been converted to **log**. Moreover the inclusion of **g=9.8m/s^2** means that **C** has the unit **√m/s.**

Hydraulic roughness is expressed in terms of the Chézy (**C**), Manning-Strickler (**n**), Darcy-Weisbach (**λ**). The relation between **C** and **λ** is:

$$C^2 = \frac{8 \cdot g}{\lambda} \tag{5.42}$$

Equation 5.39 is often written as a function of the theoretical viscous sub layer thickness **δ$_\nu$** (equation 5.33) and the hydraulic radius (**R=A/O**):

$$C = 18 \cdot \log\left(\frac{12 \cdot R}{\delta_\nu / 3.5 + k_s}\right) \tag{5.43}$$

Note that the hydraulic radius does not equal half the hydraulic diameter, but one fourth, since the hydraulic diameter **D=4·A/O**. The hydraulic diameter concept matches pipe flow, where the hydraulic diameter equals the pipe diameter for around pipe, where the hydraulic radius concept matches river flow, where for a wide river, the hydraulic radius equals the depth of the river.

Figure 43: Range of values of the roughness coefficient n for different types of channels.

In these equations k_s is the equivalent sand roughness according to Nikuradse. For an alluvial bed the value of k_s varies strongly with the flow conditions. In rivers the flow regime will often be hydraulically rough ($k_s >> d$). According to Strickler the Chézy coefficient is:

$$C = \left(\frac{R}{k_s} \right)^{1/6} \qquad (5.44)$$

Most often used, and linked with Strickler's equation, is the Manning roughness formula (or Manning-Strickler roughness formula). The relation between Manning's roughness coefficient n and the Chézy coefficient C is (with R in meters):

$$C = \frac{R^{1/6}}{n} \qquad (5.45)$$

Figure 43 gives an overview of Manning's roughness coefficient n for different types of channels. Chapter 5.3 will go into detail regarding the Darcy-Weisbach friction coefficient.

5.1.7. Drag coefficient, lift coefficient and friction coefficient.

Drag and lift coefficients

A real fluid moving past a body will exert a drag force on the body, see Figure 44.
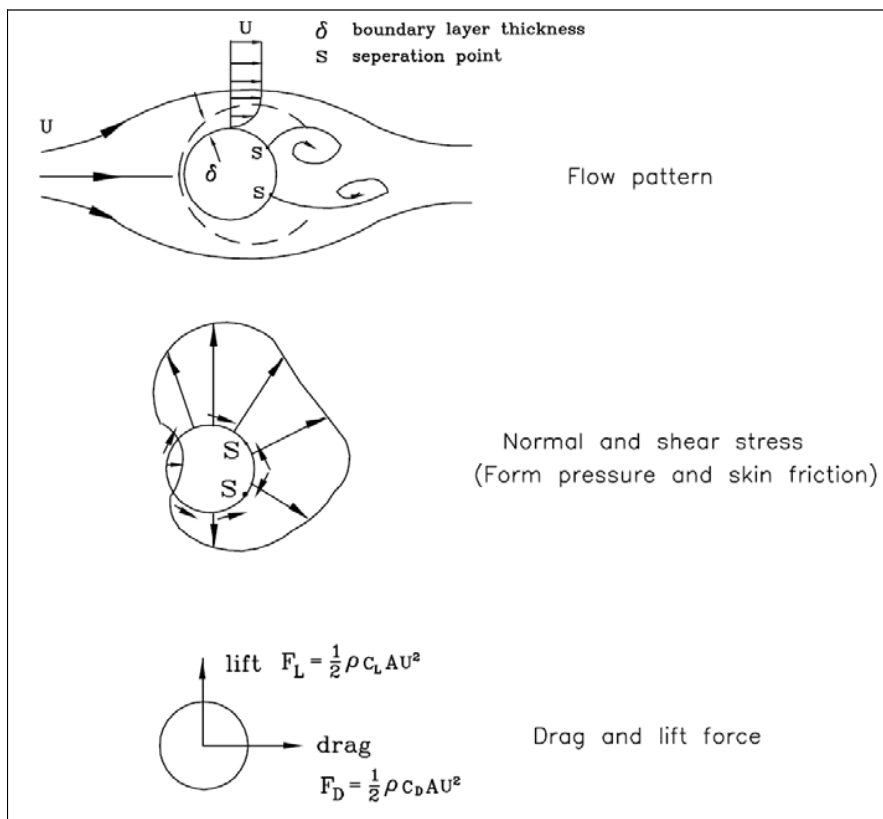
Figure 44: Drag force and lift force.

Drag force is consisted of friction drag and form drag, the former comes from the projection of skin friction force in the flow direction, and the latter from the projection of the form pressure force in the flow direction. The total drag is written as:

$$\mathbf{F_D} = \mathbf{C_D} \cdot \tfrac{1}{2} \cdot \rho \cdot \mathbf{U}^2 \cdot \mathbf{A} \tag{5.46}$$

The lift force is written in the same way:

$$\mathbf{F_L} = \mathbf{C_L} \cdot \tfrac{1}{2} \cdot \rho \cdot \mathbf{U}^2 \cdot \mathbf{A} \tag{5.47}$$

Where: **A** - Projected area of the body to the plane perpendicular to the flow direction.
  $\mathbf{C_D}$, $\mathbf{C_L}$ - Drag and lift coefficients, depend on the shape and surface roughness of the body and the Reynolds number. They are usually determined by experiments

Friction coefficient

Figure 45 illustrates fluid forces acting on a grain resting on the bed. The drag force:

$$\mathbf{F_D} = \mathbf{C_D} \cdot \tfrac{1}{2} \cdot \rho \cdot (\varsigma \cdot \mathbf{U})^2 \cdot \mathbf{A} \tag{5.48}$$

where ζ is included because we do not know the fluid velocity past the grain, but we can reasonably assume that it is the function of the average velocity and other parameters.
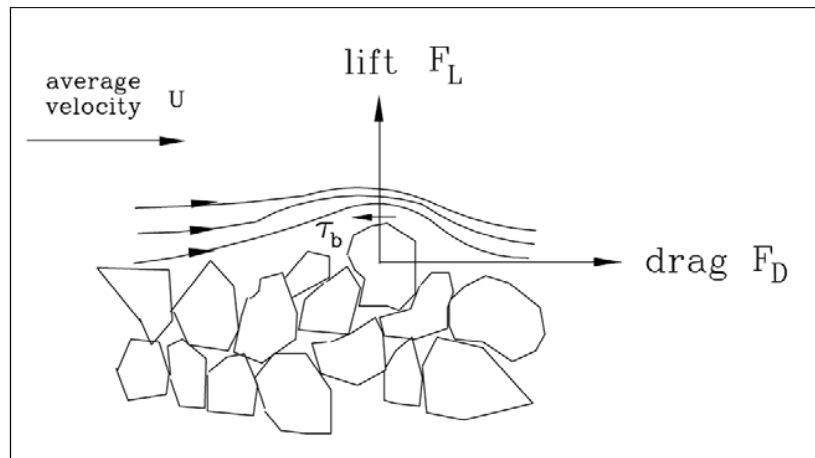
Figure 45: Fluid forces acting on a grain resting on the bed.

We can also say that the grain exerts a resistant force $\mathbf{F_D}$ on the flow. If **A'** is the projected area of the grain to the horizontal plane, the bottom shear stress is:

$$\tau_b = \frac{\mathbf{F_D}}{\mathbf{A'}} = \left(\mathbf{C_D} \cdot \varsigma^2 \cdot \frac{\mathbf{A}}{\mathbf{A'}} \right) \cdot \tfrac{1}{2} \cdot \rho \cdot \mathbf{U}^2 = \mathbf{f} \cdot \tfrac{1}{2} \cdot \rho \cdot \mathbf{U}^2 = \frac{\lambda}{4} \cdot \tfrac{1}{2} \cdot \rho \cdot \mathbf{U}^2 \tag{5.49}$$

Where: **f** is the Fanning friction (**4·f=λ**) coefficient of the bed, which is a dimensionless parameter. By applying the Chézy coefficient we get:

$$C^2 = \frac{2 \cdot g}{f} \tag{5.50}$$

$$f \approx \frac{0.06}{\left(\log\left(\frac{12 \cdot h \cdot u_*}{3.3 \cdot \nu} \right) \right)^2} \qquad \text{Hydraulically smooth flow} \qquad \frac{u_* \cdot k_s}{\nu} \leq 5 \tag{5.51}$$

$$f \approx \frac{0.06}{\left(\log\left(\frac{12 \cdot h}{k_s} \right) \right)} \qquad \text{Hydraulically rough flow} \qquad \frac{u_* \cdot k_s}{\nu} \geq 70 \tag{5.52}$$

5.2. The Camp approach.

When the height of the sediment increases and the hopper load parameter remains constant, the horizontal flow velocity above the sediment also increases. Grains that have already settled will be re-suspended and leave the basin through the overflow. This is called scouring. First the small grains will not settle or erode and when the level increases more, also the bigger grains will stop settling, resulting in a smaller settling efficiency.

The shear force of water on a spherical particle is:

$$\tau = \frac{1}{4} \cdot \lambda \cdot \frac{1}{2} \cdot \rho_w \cdot s_s^2 \tag{5.53}$$

The shear force of particles at the bottom (mechanical friction) is proportional to the submerged weight of the sludge layer, per unit of bed surface (see Figure 21):

$$f = \mu \cdot N = \mu \cdot (1-n) \cdot (\rho_q - \rho_w) \cdot g \cdot d \tag{5.54}$$

In equilibrium the hydraulic shear equals the mechanical shear and the critical scour velocity can be calculated. The scour s_s velocity for a specific grain with diameter d_s, according to Huisman (1995) and Camp (1946) is:

$$s_s = \sqrt{\frac{8 \cdot \mu \cdot (1-n) \cdot (\rho_q - \rho_w) \cdot g \cdot d_s}{\lambda \cdot \rho_w}} \tag{5.55}$$

Grains that are re suspended due to scour, will not stay in the basin and thus have a settling efficiency of zero. In this equation, λ is the viscous friction coefficient mobilized on the top surface of the sediment and has a value in the range of 0.01-0.03, depending upon the Reynolds number and the ratio between the hydraulic radius and the grain size (surface roughness). The porosity n has a value in the range 0.4-0.5, while the friction coefficient μ depends on the internal friction of the sediment and has a value in the range of 0.1-1.0 for sand grains.
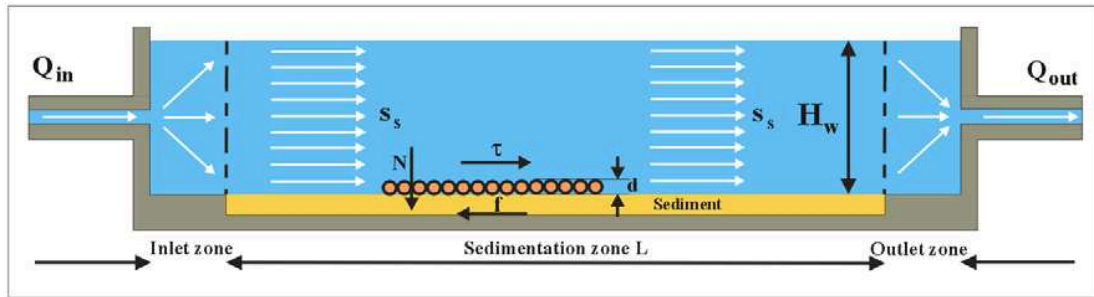
Figure 46: The equilibrium of forces on a particle.

With **µ·(1-n)=0.05** and **λ=0.03** this gives:

$$s_s = \sqrt{\frac{40 \cdot (\rho_q - \rho_w) \cdot g \cdot d_s}{3 \cdot \rho_w}} \qquad (5.56)$$

The particle diameter of particles that will not settle due to scour (and all particles with a smaller diameter) is:

$$d_s = \frac{3 \cdot \rho_w}{40 \cdot (\rho_q - \rho_w) \cdot g} \cdot s_s^2 \qquad (5.57)$$

Knowing the diameter d_s, the fraction p_s that will not settle due to scour can be found if the PSD of the sand is known. Equation 5.56 is often used for designing settling basins for drinking water. In such basins scour should be avoided, resulting in an equation with a safety margin. For the prediction of the erosion during the final phase of the settling process in TSHD's a more accurate prediction of the scour velocity is required.

5.3.   The Shields approach.

Let us consider the steady flow over the bed composed of cohesion less grains. The forces acting on the grain is shown in Figure 47.
The driving force is the flow drag force on the grain, assuming that part of the surface of the particle is hiding behind other particles and only a fraction **β** is subject to drag and lift:

$$F_D = C_D \cdot \tfrac{1}{2} \cdot \rho_w \cdot (\alpha \cdot u_*)^2 \cdot \beta \cdot \frac{\pi \cdot d^2}{4} \qquad (5.58)$$

The lift force is written in the same way:

$$F_L = C_L \cdot \tfrac{1}{2} \cdot \rho_w \cdot (\alpha \cdot u_*)^2 \cdot \beta \cdot \frac{\pi \cdot d^2}{4} \qquad (5.59)$$

The submerged weight of the particle is:

$$F_w = (\rho_q - \rho_w) \cdot g \cdot \frac{\pi \cdot d^3}{6} \qquad (5.60)$$
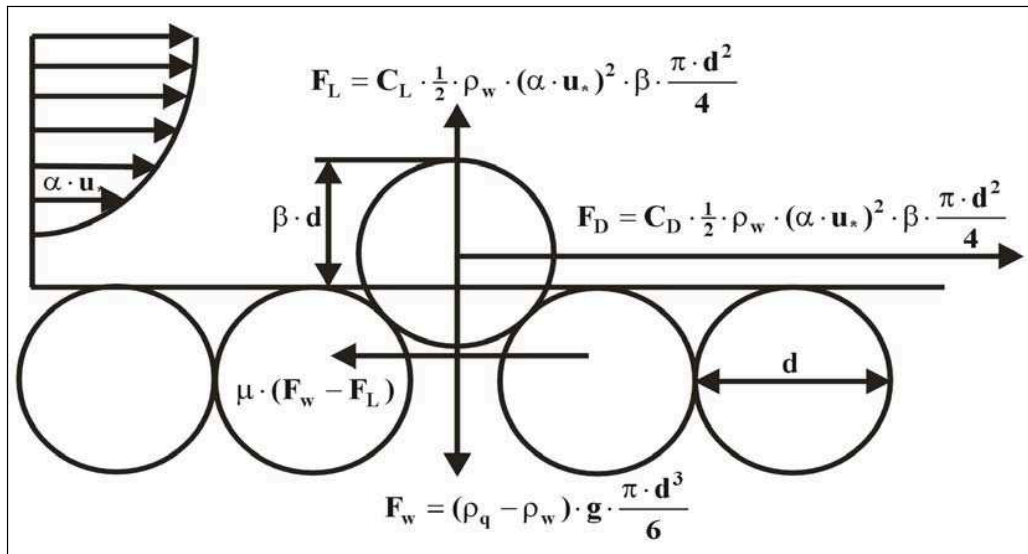
Figure 47: Forces acting on a grain resting on the bed.

At equilibrium:

$$\mathbf{F_D} = \mu \cdot (\mathbf{F_w} - \mathbf{F_L})$$
(5.61)

where the friction velocity $\mathbf{u_*}$ is the flow velocity close to the bed. $\boldsymbol{\alpha}$ is a coefficient, used to modify $\mathbf{u_*}$ so that $\boldsymbol{\alpha}\mathbf{u_*}$ forms the characteristic flow velocity past the grain. The stabilizing force can be modeled as the friction force acting on the grain. If $\mathbf{u_{*,c}}$, critical friction velocity, denotes the situation where the grain is about to move, then the drag force is equal to the friction force, so:

$$C_D \cdot \tfrac{1}{2} \cdot \rho_w \cdot (\alpha \cdot u_{*,c})^2 \cdot \beta \cdot \frac{\pi \cdot d^2}{4} = \mu \cdot \left((\rho_q - \rho_w) \cdot g \cdot \frac{\pi \cdot d^3}{6} - C_L \cdot \tfrac{1}{2} \cdot \rho_w \cdot (\alpha \cdot u_{*,c})^2 \cdot \beta \cdot \frac{\pi \cdot d^2}{4} \right)$$
(5.62)

Which can be re-arranged into:

$$\frac{u_{*,c}^2}{R_d \cdot g \cdot d} = \frac{4}{3} \cdot \frac{1}{\alpha^2} \cdot \frac{\mu}{\beta \cdot C_D + \mu \cdot \beta \cdot C_L}$$
(5.63)

The Shields parameter is now defined as:

$$\theta_c = \frac{u_{*,c}^2}{R_d \cdot g \cdot d}$$
(5.64)

Re-arranging gives a simple equation for the Shields parameter:

$$\theta_c = \frac{u_{*,c}^2}{R_d \cdot g \cdot d} = \frac{4}{3} \cdot \frac{\mu}{\beta} \cdot \frac{1}{\alpha^2} \cdot \frac{1}{C_D + \mu \cdot C_L}$$
(5.65)

Since $\mathbf{C_D}$ normally depends on the boundary Reynolds number $\mathbf{Re_*}$, the Shields $\mathbf{\theta_c}$ number will be a function of the boundary Reynolds number $\mathbf{Re_*=u_* \cdot d/v}$. Carrying out an equilibrium of moments around the contact point of a particle with the particle its resting on, results in the same equation. One can discuss which equation to use for the $\mathbf{C_D}$ value and the $\mathbf{C_L}$ value, since the particles are not free from the surface as with the determination of the settling velocity for individual particles, but for a first approximation equation 4.9 will be used.

Now the question is, what would such a function look like. Figure 48 shows the relation between the Shields parameter and the boundary Reynolds number as is shown in Shields (1936).
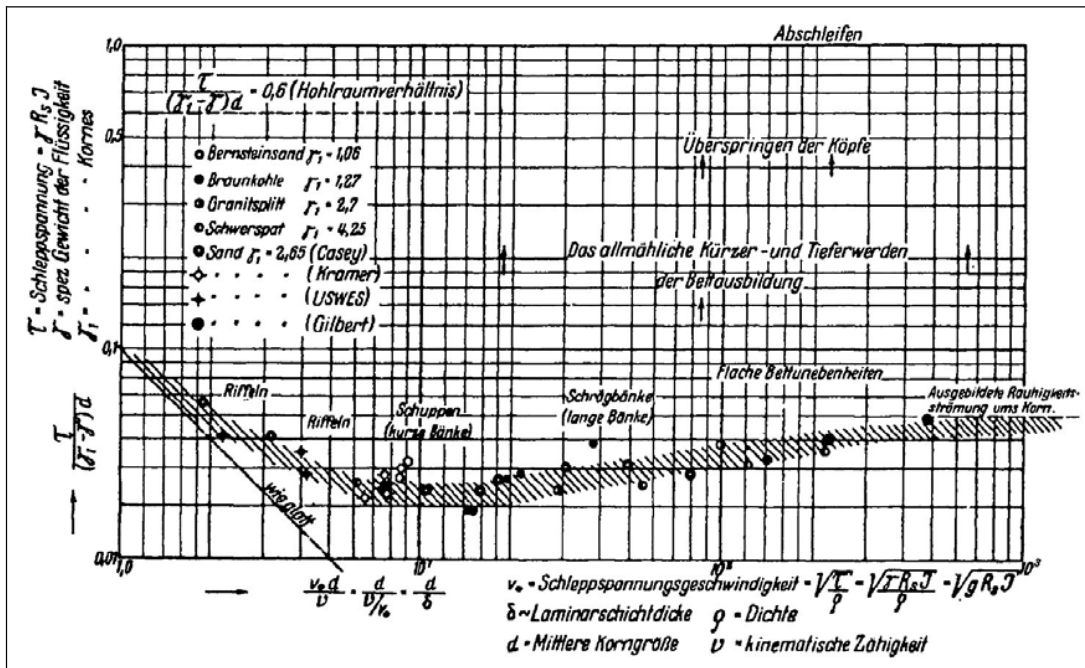
Figure 48: The original Shields (1936) curve.

It is however interesting to investigate if this curve can be determined in a more fundamental way. Based on the theory in this chapter the following can be derived.

Case 1: Hydraulically smooth flow (very low Re*).

First lets assume a very small particle in a viscous laminar boundary layer. The particle is hiding for **(1- β)** behind other particles, which also means that **β** of the surface is subject to drag, assume **β** is about 0.5, which means the changes in drag area are about proportional with **β**. According to equation 5.32 the velocity **u(z)** in the viscous sub layer at **β** times the diameter **d** height is equal to:

$$\mathbf{u(\beta \cdot d) = \frac{u_*^2}{v} \cdot \beta \cdot d} \tag{5.66}$$

Since the velocity develops linear with z, the drag force exerted on the particle, has to be found by integration of the velocity squared over the surface that is subject to the drag, but since the shape of the particle is not a square, but irregular, an effective velocity of

$\frac{1}{3} \cdot \sqrt{3} = 0.577$ of the velocity at the top of the particle is chosen. This gives for the effective velocity on the particle:

$$\mathbf{u_{eff}} = \tfrac{1}{3} \cdot \sqrt{3} \cdot \mathbf{u}(\beta \cdot \mathbf{d}) = \tfrac{1}{3} \cdot \sqrt{3} \cdot \frac{\mathbf{u_*^2}}{\mathbf{\nu}} \cdot \beta \cdot \mathbf{d} = \tfrac{1}{3} \cdot \sqrt{3} \cdot \beta \cdot \frac{\mathbf{u_*^2}}{\mathbf{\nu}} \cdot \mathbf{d} \qquad (5.67)$$

With:

$$\mathbf{u_{eff}} = \alpha \cdot \mathbf{u_*} = \tfrac{1}{3} \cdot \sqrt{3} \cdot \beta \cdot \frac{\mathbf{u_*}}{\mathbf{\nu}} \cdot \mathbf{d} \cdot \mathbf{u_*} \qquad (5.68)$$

So the coefficient α is equal to:

$$\alpha = \tfrac{1}{3} \cdot \sqrt{3} \cdot \beta \cdot \frac{\mathbf{u_*}}{\mathbf{\nu}} \cdot \mathbf{d} = \tfrac{1}{3} \cdot \sqrt{3} \cdot \beta \cdot \mathbf{Re_*} \qquad (5.69)$$

The Reynolds number for the flow around the particle is, assuming the hydraulic diameter of the particle equals 4 times the area that is subject to drag, divided by the wetted perimeter equals **d**:

$$\mathbf{Re_p} = \frac{\mathbf{u_{eff}} \cdot \mathbf{d}}{\mathbf{\nu}} = \tfrac{1}{3} \cdot \sqrt{3} \cdot \beta \cdot \left(\frac{\mathbf{u_*} \cdot \mathbf{d}}{\mathbf{\nu}} \right)^2 = \tfrac{1}{3} \cdot \sqrt{3} \cdot \beta \cdot \mathbf{Re_*^2} = \alpha \cdot \mathbf{Re_*} \qquad (5.70)$$

The drag coefficient in this Stokes area equals, as already mentioned in chapter 4.:

$$\mathbf{C_D} = \frac{\mathbf{24}}{\mathbf{Re_p}} \qquad (5.71)$$

Substituting this in equation 5.65 gives for the Shields parameter:

$$\theta_c = \frac{\mathbf{4}}{\mathbf{3}} \cdot \frac{\mu}{\beta} \cdot \left(\frac{\mathbf{1}}{\tfrac{1}{3} \cdot \sqrt{3} \cdot \beta \cdot \mathbf{Re_*}} \right)^2 \cdot \frac{\tfrac{1}{3} \cdot \sqrt{3} \cdot \beta \cdot \mathbf{Re_*^2}}{\mathbf{24}} = \frac{\sqrt{3}}{\mathbf{18}} \cdot \frac{\mu}{\beta^2} \qquad (5.72)$$

Lets assume a mechanical friction coefficient of $\mu=0.5$ and a surface factor $\beta=0.5$ (meaning that 50% of the particle is subject to drag). This would give a Shields parameter of 0.19. Soulsby & Whitehouse (1997) assume there is a maximum of 0.3, but as can be concluded from equation 5.72, there must be a certain bandwidth depending on the mechanical friction coefficient μ and the fraction of the surface of the particle that is subject to drag β. Using equation 4.9 for the transition region for $\mathbf{C_D}$, gives:

$$\theta_c = \frac{\mathbf{4}}{\mathbf{3}} \cdot \frac{\mu}{\beta} \cdot \left(\frac{\mathbf{1}}{\tfrac{1}{3} \cdot \sqrt{3} \cdot \beta \cdot \mathbf{Re_*}} \right)^2 \cdot \frac{\mathbf{1}}{\dfrac{\mathbf{24}}{\tfrac{1}{3} \cdot \sqrt{3} \cdot \beta \cdot \mathbf{Re_*^2}} + \dfrac{\mathbf{3}}{\left(\tfrac{1}{3} \cdot \sqrt{3} \cdot \beta \cdot \mathbf{Re_*^2} \right)^{0.5}} + 0.34} \qquad (5.73)$$

Case 2: Hydraulically rough flow (very high Re*).

Now lets consider a very course particle in turbulent flow. According to equation 5.26 the velocity equals to:

$$u(z) = \frac{u_*}{\kappa} \cdot \ln\left(\frac{z}{0.033 \cdot k_s}\right) \qquad (5.74)$$

Assuming a roughness k_s about equal to β times the particle diameter d, gives:

$$u(\beta \cdot d) = \frac{u_*}{\kappa} \cdot \ln\left(\frac{1}{0.033}\right) = 8.53 \cdot u_* \qquad (5.75)$$

The effective velocity will be smaller, but since the particle is subject to turbulent flow in a logarithmic velocity field, equation 5.74 should be used to determine the effective velocity the part of the particle subject to drag, with respect to drag. For a logarithmic velocity field this is 0.764 times the velocity at the top of the particle, giving a velocity coefficient **α=6.5,** resulting in an effective velocity of:

$$u_{eff} = 6.5 \cdot u_* \qquad (5.76)$$

And a particle Reynolds number of:

$$Re_p = \frac{u_{eff} \cdot d}{\nu} = 6.5 \cdot \frac{u_* \cdot d}{\nu} = 6.5 \cdot Re_* = \alpha \cdot Re_* \qquad (5.77)$$

The drag coefficient C_D has a constant value of 0.445 for turbulent flow as described in chapter 4. Substituting this in equation 5.65 gives:

$$\theta_c = \frac{4}{3} \cdot \frac{\mu}{\beta} \cdot \frac{1}{6.5^2} \cdot \frac{1}{0.445} = 0.0709 \cdot \frac{\mu}{\beta} \qquad (5.78)$$

If the mechanical friction coefficient μ and the area coefficient β are chosen equal, this results in a Shields parameter θ_c of about 0.071 for the very high Reynolds Re_* numbers. In literature a value of 0.055-0.060 is found, but measurements show a certain bandwidth. Using a mechanical friction coefficient μ of 0.45 and an area factor β of 0.55, results in a Shields parameter θ_c of 0.058, which matches literature. Values smaller then 0.5 for the area factor β are unlikely, because the Shields parameters predicts the beginning of erosion/scour of the entire sediment and there will always be particles with a higher area factor β up to about 0.75. Using this maximum area factor with a mechanical friction coefficient μ of 0.45, gives a Shields parameter θ_c of about 0.0425. Using equation 4.9 for the transition region, gives:

$$\theta_c = \frac{4}{3} \cdot \frac{\mu}{\beta} \cdot \left(\frac{1}{6.5}\right)^2 \cdot \frac{1}{\dfrac{24}{(6.5 \cdot Re_*)} + \dfrac{3}{(6.5 \cdot Re_*)^{0.5}} + 0.34} \qquad (5.79)$$

Case 3: Transitional flow (medium Re∗).

In the transitional area, both the linear velocity profile of the viscous sub layer and the logarithmic profile play a role in the forces on a particle. The transitional area has no fixed boundaries, but roughly its from **Re∗=0.5** to **Re∗=20.** For the transitional area an empirical equation can be used for the velocity profile, according to:

$$\alpha = A - B \cdot e^{-C \cdot Re_*^{D}}$$
$$A = 5.62 + 0.70 \cdot \beta$$
$$B = 5.62 + 0.68 \cdot \beta \quad\quad\quad\quad\quad (5.80)$$
$$C = 0.063 - 0.0237 \cdot \beta$$
$$D = 1.488 - 0.1183 \cdot \beta$$

With:

$$Re_p = \alpha \cdot Re_* \quad\quad\quad\quad\quad (5.81)$$

Using equation 4.9 for the transition region for **C$_D$**, and equation 5.63, the Shields curve can be determined. Figure 49 shows the estimated curves for values of **β** of 0.475, 0.525, 0.6, 0.7, 0.8, 0.9 and 1.0, with in the back ground the original Shields curve, while Figure 50 shows these with in the background measured values of the Shields parameter from Julien (1995). The estimated curves are calculated with a friction coefficient **μ=0.45** and a lift coefficient **C$_L$=0.25**. It is very well possible that in reality this coefficient may have a higher value. It is also possible that this coefficient depends on the particle diameter or the particle Reynolds number.
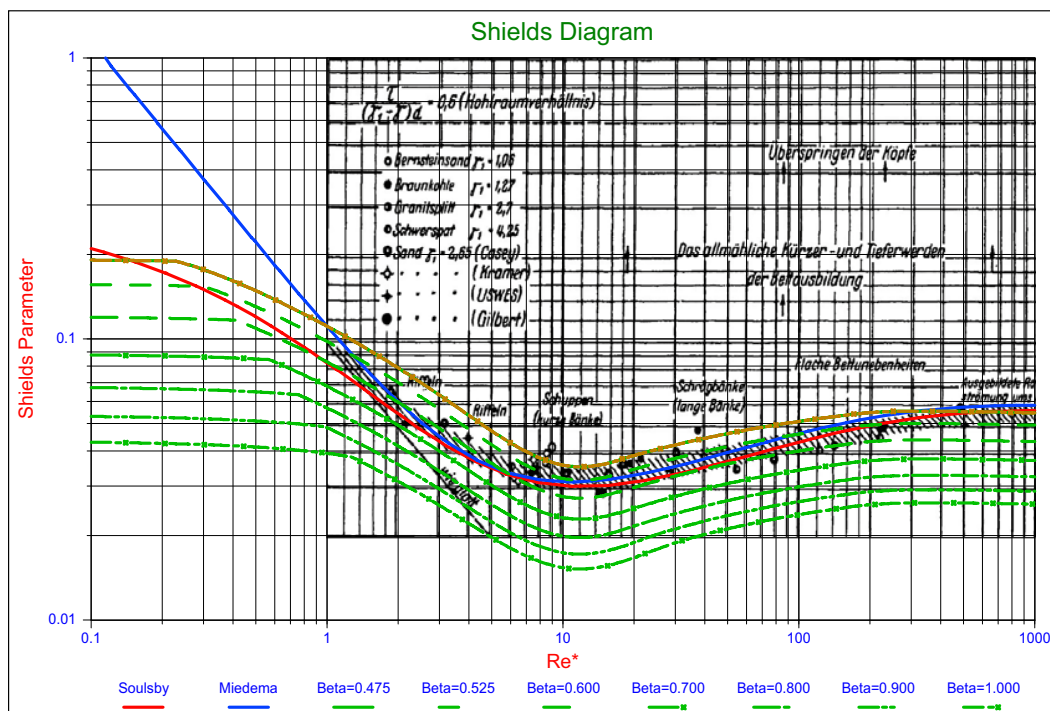
Figure 49: The estimated Shields curves versus the original Shields curve.
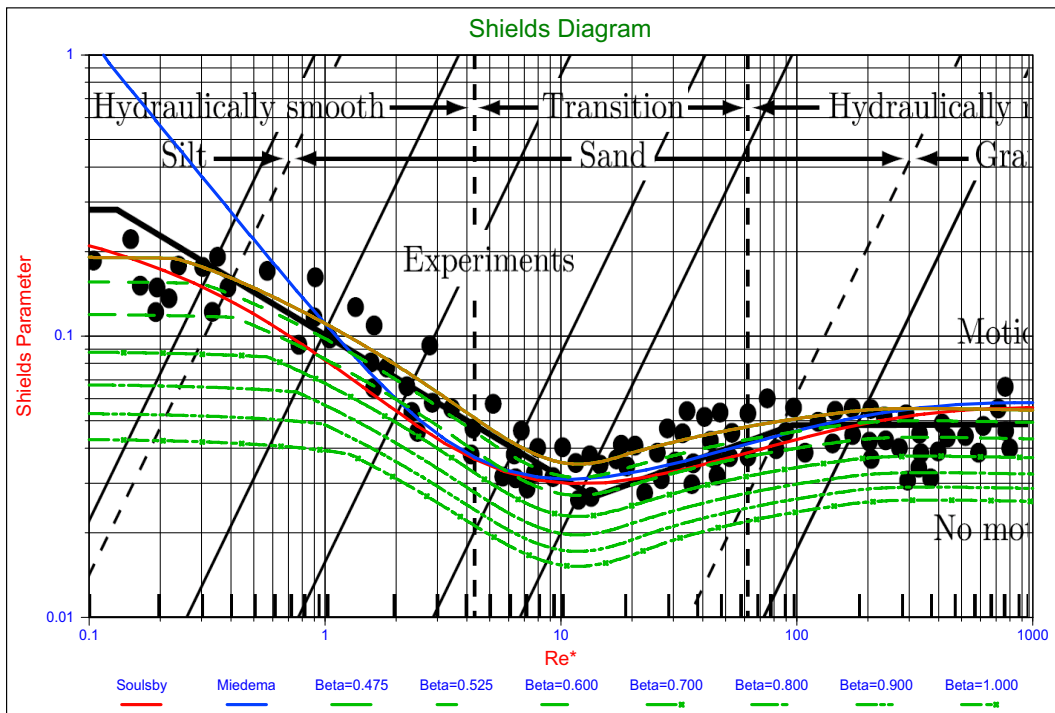
Figure 50: The estimated Shields curves for different values of β.
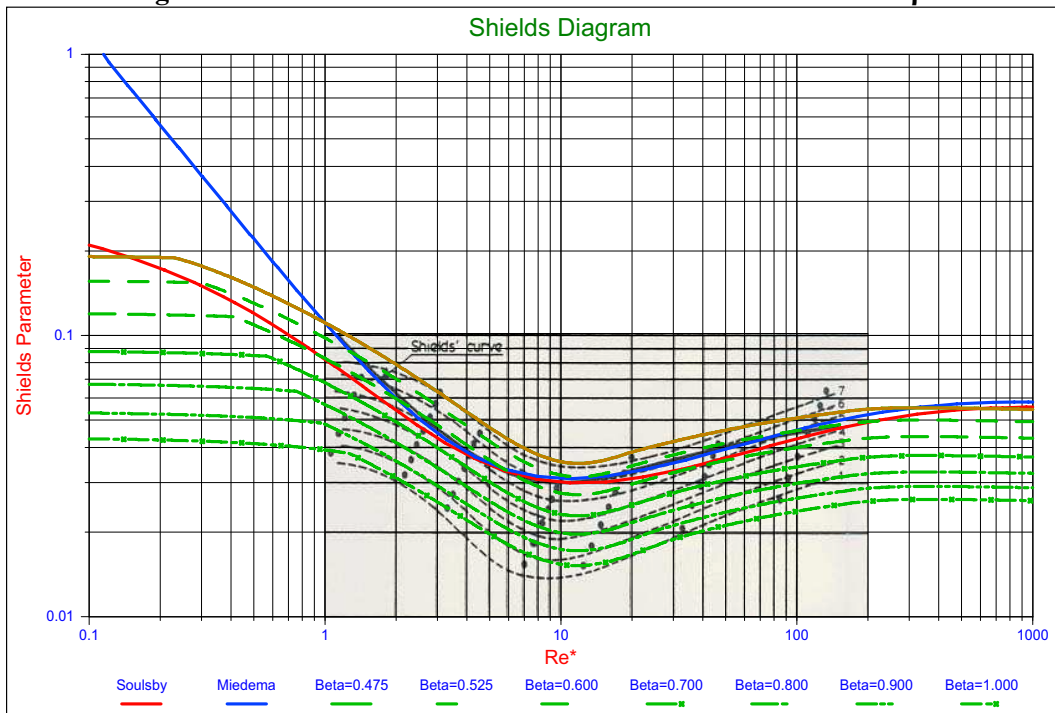
Figure 51: The 7 levels of erosion according to Delft Hydraulics (1972).

The Delft Hydraulics (1972) defined 7 levels of erosion according to:
1. Occasional particle movement at some locations.
2. Frequent particle movement at some locations.
3. Frequent particle movement at many locations.
4. Frequent particle movement at nearly all locations.

5. Frequent particle movement at all locations.
6. Permanent particle movement at all locations.
7. General transport (initiation of ripples).

As can be seen from Figure 51, the curves with the 7 values for **β** match closely with the 7 levels according to Delft Hydraulics (1972), although there are differences. Since the factor **β** is the fraction of a particle that is subject to drag, this seems plausible. In a normal sediment, there will be a few particles that lay on top of the bed and that are subject to drag for 100%. These particles will be the first to move (erode), so this is level 1. Particles that are embedded for 50% will be much harder to move and form level 5 or higher.

5.4. Shields approximation equations.

Many researchers created equations to approximate the Shields curve. The original Shields graph however is not convenient to use, because both axis contain the shear velocity **u**∗ and this is usually an unknown, this makes the graph an implicit graph. To make the graph explicit, the graph has to be transformed to another axis system. In literature often the dimensionless grain diameter **D**∗ is used. This dimensionless diameter has already been used in equation 4.34 for the Grace method for determining the settling velocity, assuming the water density equals 1. This dimensionless diameter also called the Bonneville parameter is:

$$\mathbf{D_* = d \cdot \sqrt[3]{\frac{R_d \cdot g}{\nu^2}}} \tag{5.82}$$
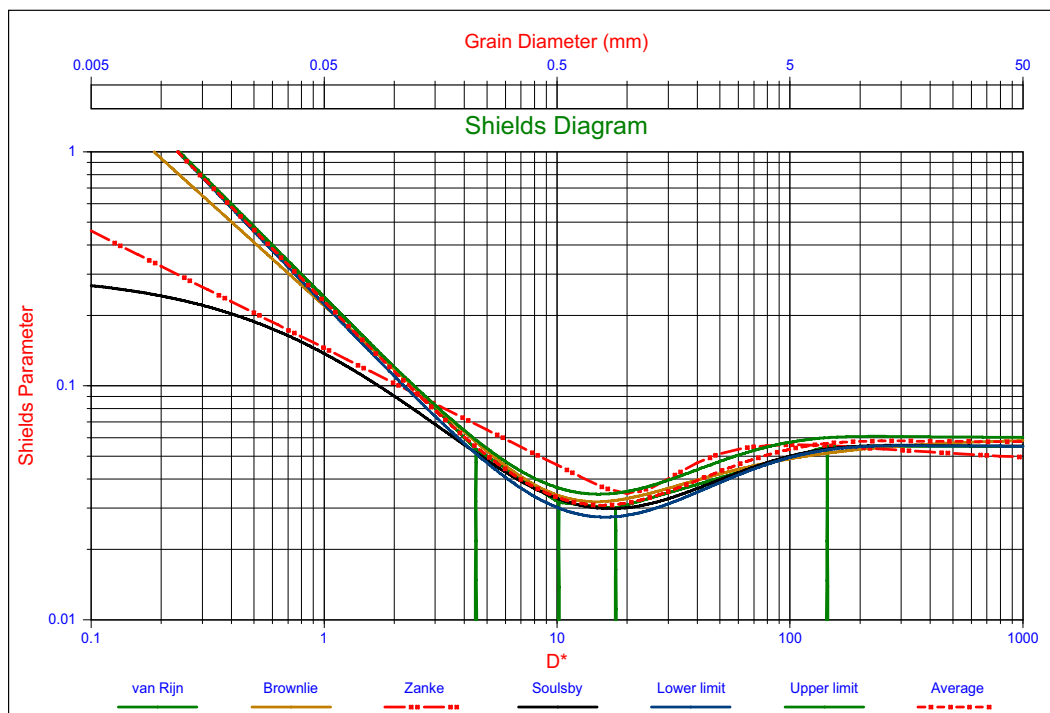
Figure 52: The Shields parameter as a function of the dimensionless diameter.

With the normal values for the water density, the relative density and the viscosity, the dimensionless diameter is about 20.000 times the particle diameter, or 20 times the particle

diameter in mm. Figure 52 & Figure 53 show the Shields approximations of van Rijn (1993), Brownlie (1981), Zanke (2003), Soulsby & Whitehouse ((1997) completed with a lower limit, upper limit and average approximation derived for these lecture notes by the author. It is interesting to see that the van Rijn and Brownlie equations result in a continuously increasing Shields parameter with a decreasing dimensionless diameter, the Zanke approach does this also, but less steep, while the Soulsby & Whitehouse approach has a limit of 0.3 for very small particles, matching the model as described in the previous chapter. Only Soulsby & Whitehouse take the linear velocity profile in the viscous sub layer, resulting in a constant Shields parameter at very low Reynolds numbers, into account.
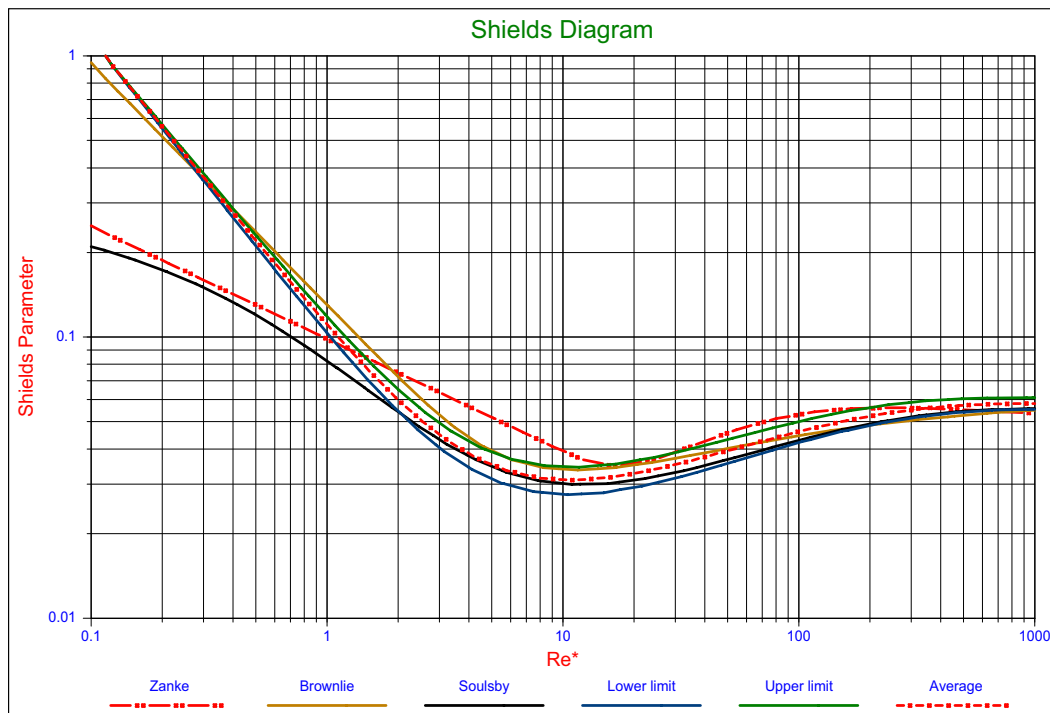
Figure 53: The Shields parameter as a function of the boundary Reynolds number.

From the definition of the Shields parameter, the relation between the Shields parameter and the Bonneville parameter can be derived, the Shields parameter is:

$$\theta_{cr} = \frac{u_*^2}{R_d \cdot g \cdot d} \tag{5.83}$$

The grain Reynolds number **Re***, which defines the transition between hydraulic smooth and rough conditions for which grains protrude into the flow above the laminar sub layer **δ** at **Re*=11.63** as:

$$Re_* = \frac{u_* \cdot d}{\nu} = \frac{\sqrt{\theta} \cdot \sqrt{R_d \cdot g \cdot d} \cdot d}{\nu} \tag{5.84}$$

Using equation 5.82, this gives:

$$\mathbf{Re_*} = \sqrt{\theta} \cdot \mathbf{D_*^{1.5}} \tag{5.85}$$

So the Bonneville parameter is a function of the Shields number and the boundary Reynolds number according to:

$$\mathbf{D_*} = \left(\frac{\mathbf{Re_*}}{\sqrt{\theta}} \right)^{2/3} \tag{5.86}$$

Another parameter that is often used for the horizontal axis is the so called Grant and Madsen (1976) parameter or sediment fluid parameter, see Figure 54:

$$\mathbf{S_*} = \frac{\sqrt{\mathbf{R_d \cdot g \cdot d} \cdot \mathbf{d}}}{4 \cdot \nu} = \frac{\mathbf{D_*^{1.5}}}{4} = \frac{\mathbf{Re_*}}{4 \cdot \sqrt{\theta}} \tag{5.87}$$

The factor of 4 appears in the definition of $\mathbf{S_*}$ to render the numerical values of $\mathbf{S_*}$ comparable with the $\mathbf{Re_*}$ values in the traditional Shields diagram. This is done merely for convenience and has no physical significance.
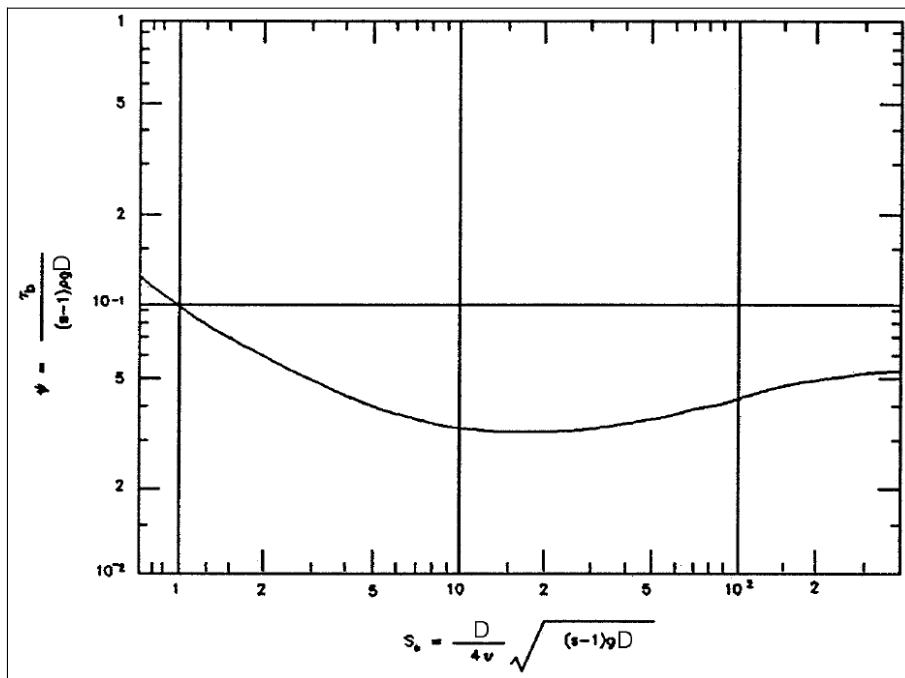
Figure 54: Modified Shields diagram, Madsen & Grant (1976).

Which differs a factor 4 from the particle Reynolds number $\mathbf{Re_p}$:

$$\mathbf{Re_p} = \frac{\sqrt{\mathbf{R_d \cdot g \cdot d} \cdot \mathbf{d}}}{\nu} = \mathbf{D_*^{1.5}} = \frac{\mathbf{Re_*}}{\sqrt{\theta}} \tag{5.88}$$

This particle Reynolds number can be derived from equations 4.5 and 4.6, omitting the constants and assuming turbulent settling with a constant drag coefficient $\mathbf{C_D}$.
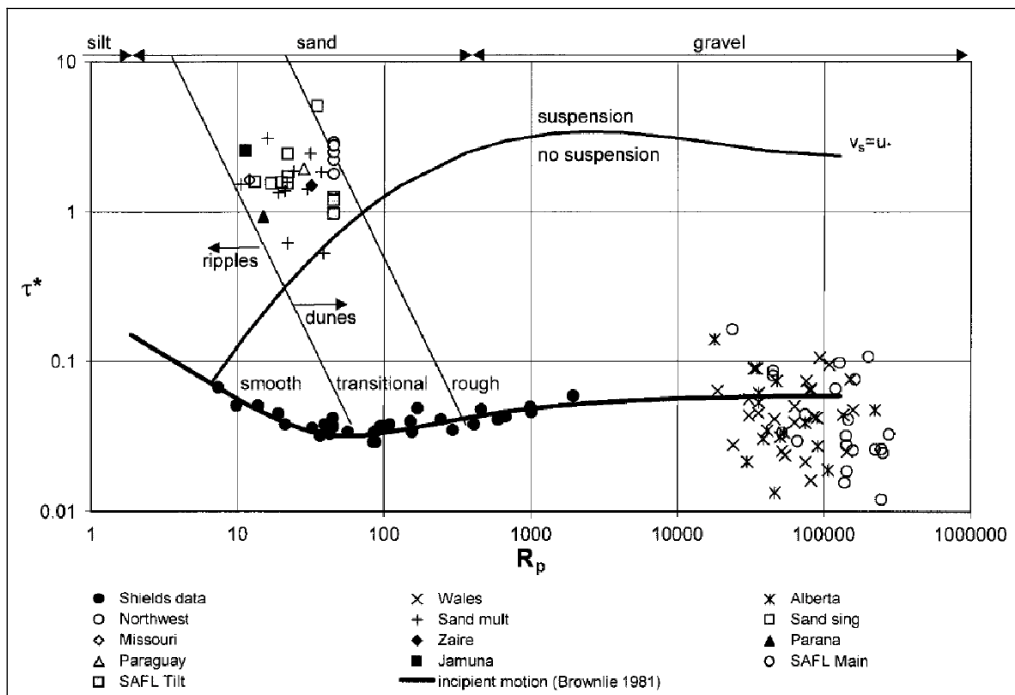
Figure 55: Modified Shields diagram using Re$_p$ (equation 5.88).

Figure 56 shows the relation between the boundary or grain Reynolds number, the Bonneville parameter (dimensionless grain diameter) and the Grant & Madsen parameter.
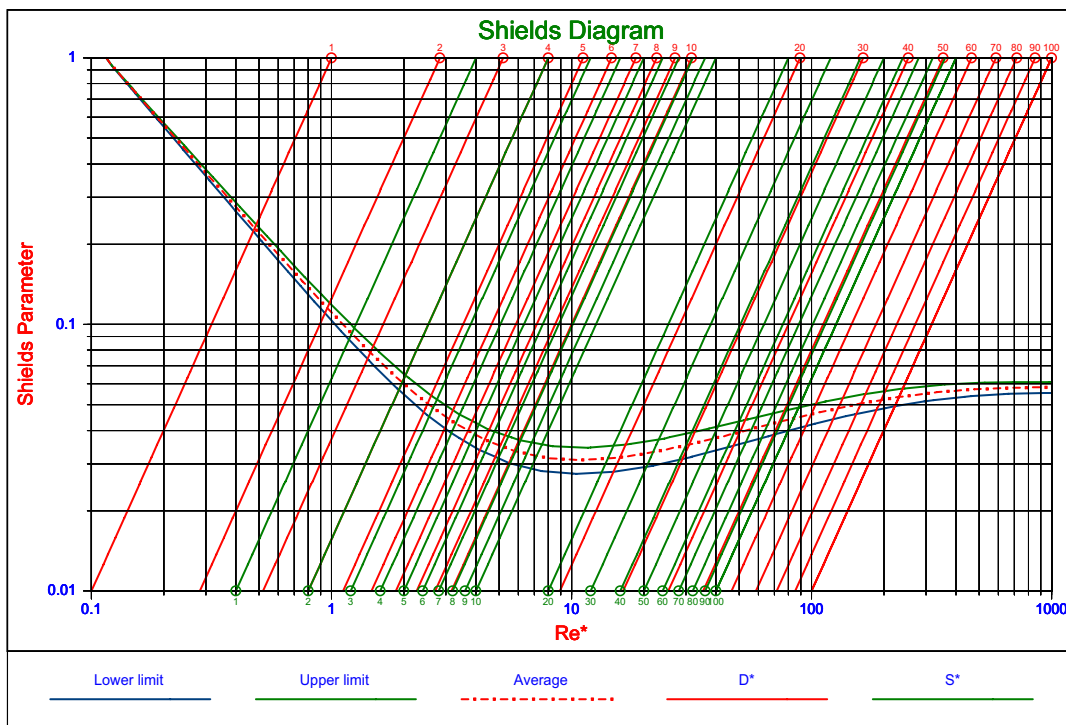
Figure 56: The relation between the boundary Reynolds number, the Bonneville parameter and the Grant and Madsen parameter.

The different approximation equations are summarized below.

$$\theta_{cr} = \frac{0.30}{(1 + 1.2 \cdot D_*)} + 0.055 \cdot \left(1 - e^{-0.02 \cdot D_*}\right) \qquad \text{Soulsby \& Whitehouse} \qquad (5.89)$$

$$\theta_{cr} = \frac{0.22}{D_*^{0.9}} + 0.06 \cdot 10^{-7.7 \cdot D_*^{-0.9}} \qquad \text{Brownlie} \qquad (5.90)$$

$$\theta_{cr} = \frac{0.24}{D_*} \qquad D_* < 4.5$$

$$\theta_{cr} = \frac{0.14}{D_*^{0.64}} \qquad 4.5 < D_* < 10.2$$

$$\theta_{cr} = \frac{0.04}{D_*^{0.1}} \qquad 10.2 < D_* < 17.9 \qquad \text{van Rijn} \qquad (5.91)$$

$$\theta_{cr} = 0.013 \cdot D_*^{0.29} \qquad 17.9 < D_* < 145$$

$$\theta_{cr} = 0.055 \qquad 145 < D_*$$

$$\theta_{cr} = \frac{0.145}{D_*^{0.5}} + 0.045 \cdot 10^{-1100 \cdot D_*^{-2.25}} \qquad \text{Zanke} \qquad (5.92)$$

$$\theta_{cr} = \frac{0.2220}{D_*^{1.04}} + 0.0550 \cdot \left(1 - e^{-0.0200 \cdot D_*}\right) \qquad \text{Miedema lower limit} \qquad (5.93)$$

$$\theta_{cr} = \frac{0.2350}{D_*^{1.00}} + 0.0600 \cdot \left(1 - e^{-0.0250 \cdot D_*}\right) \qquad \text{Miedema upper limit} \qquad (5.94)$$

$$\theta_{cr} = \frac{0.2285}{D_*^{1.02}} + 0.0575 \cdot \left(1 - e^{-0.0225 \cdot D_*}\right) \qquad \text{Miedema average} \qquad (5.95)$$

5.5. The Hjulstrom approach.

The **Hjulstrøm curve** is a graph used by hydrologists to determine whether a river will erode, transport or deposit sediment. The graph takes sediment size and channel velocity into account. The x-axis shows the size of the particles in mm. The y-axis shows the velocity of the river in cm/s. The tree lines on the diagram show when different sized particles will be deposited, transported or eroded. The Curve uses a double logarithmic scale.

The curve shows several key ideas about the relationships between erosion, transportation and deposition. The Hjulstrøm Curve shows that particles of a size around 1mm require the least energy to erode, as they are sands that do not coagulate. Particles smaller than these fine sands are often clays which require a higher velocity to produce the energy required to split the small clay particles which have coagulated. Larger particles such as pebbles are eroded at higher velocities and very large objects such as boulders require the highest velocities to erode. When the velocity drops below this velocity called the *line of critical velocity*, particles will be deposited or transported, instead of being eroded, depending on the river's energy.

Threshold of Motion

Grains forming the boundary between a fluid and a sediment possess a finite weight and finite coefficient of friction. When the applied shear stress is low they are not brought into motion. As applied shear stress is increased, a critical shear stress is reached at which grains will begin to move. The value of the critical stress will depend primarily on the size and density of the particles and secondarily on their shape and packing and the cohesive forces acting between particles.
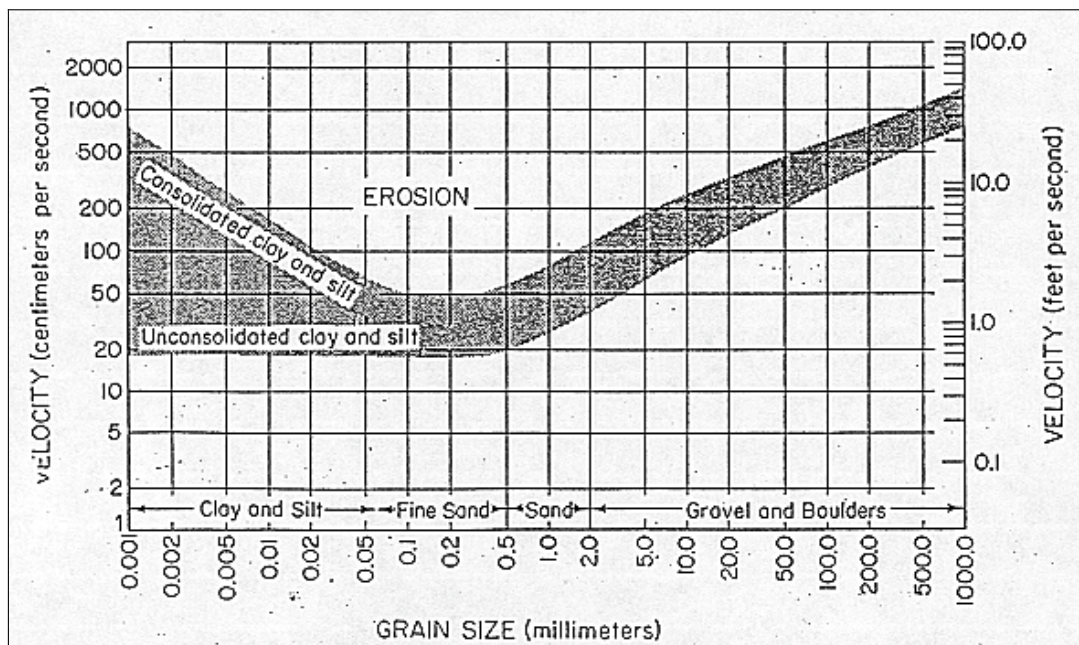
One the critical stress is just exceeded, particles will advance in the direction of flow due to irregular jumps or less commonly rolls. This mode of transport is termed the bed load and

conceptually can be thought of as being deterministic, that is the behavior of a particle once in motion is dominated by the gravity force. As the stress is further increased, particles will also begin to be suspended in solution and subject to turbulent forces. This mode of transport is termed the suspended load. Due to these two modes of transport there will be a flux of material across a plane perpendicular to the flow. Our ultimate goal is to determine this mass flux by integrating the product of the velocity profile and concentration profile.

The Critical Stress

The motion of sediment can be parameterized in a number of ways. The oldest of these is due to Hjulstrom who summarized observational data in terms of fluid velocity and grain size.

There are a number of variants of the Hjulstrom diagram, using grain diameter as one parameter and some measure of the stress as the other (via the quadratic stress law: u, u_{100} or stress itself: u_*):
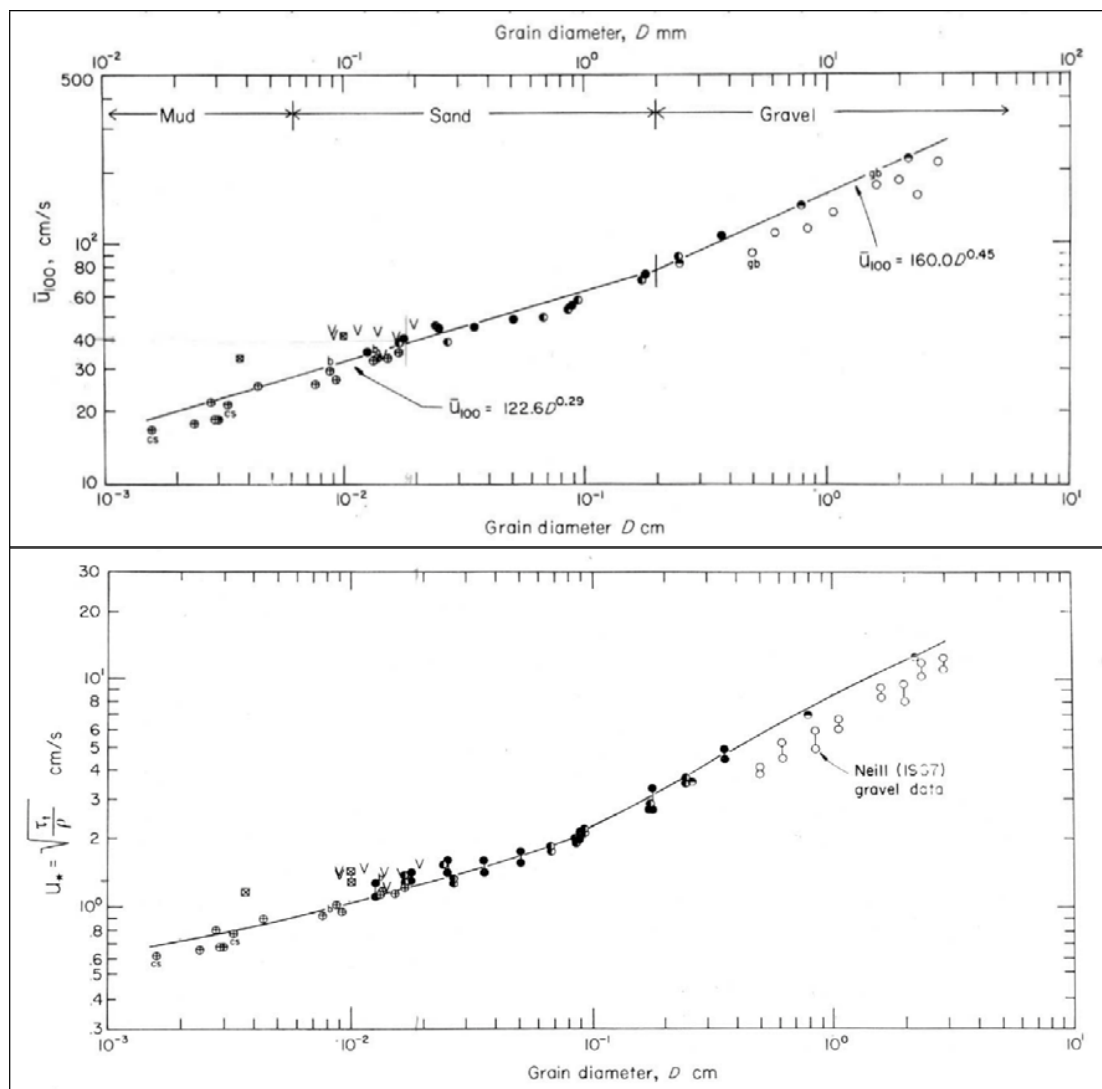
In several of these figures there is a envelope of values for small particles, contrasting unconsolidated and consolidated/cohesive sediment. This reflects the importance of inter particle forces because of the higher ratio of surface area to volume.

Sundborg (1956) - added more detail, and dealt with consolidation in fine-grained end.
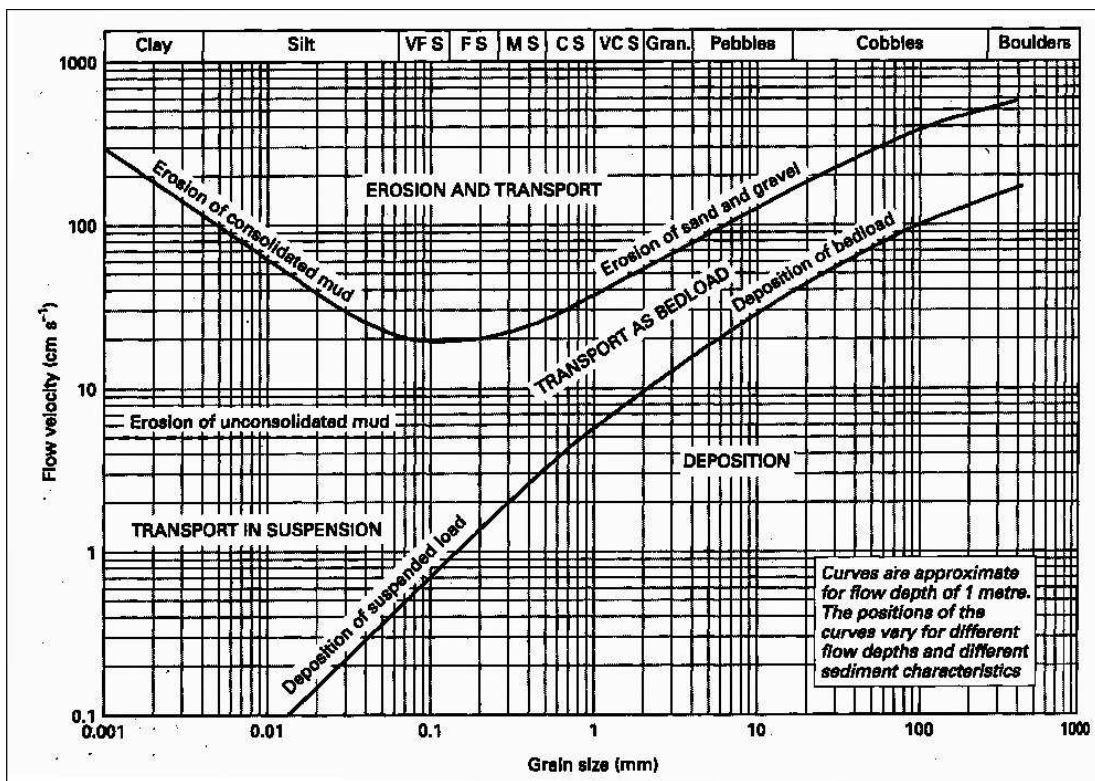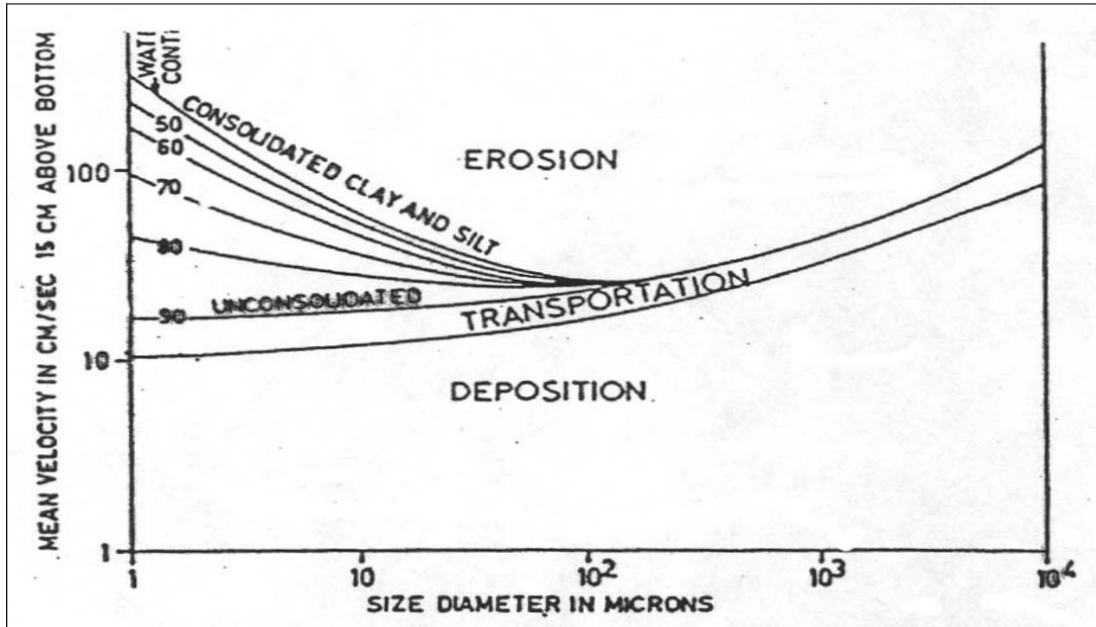
Figure 57:
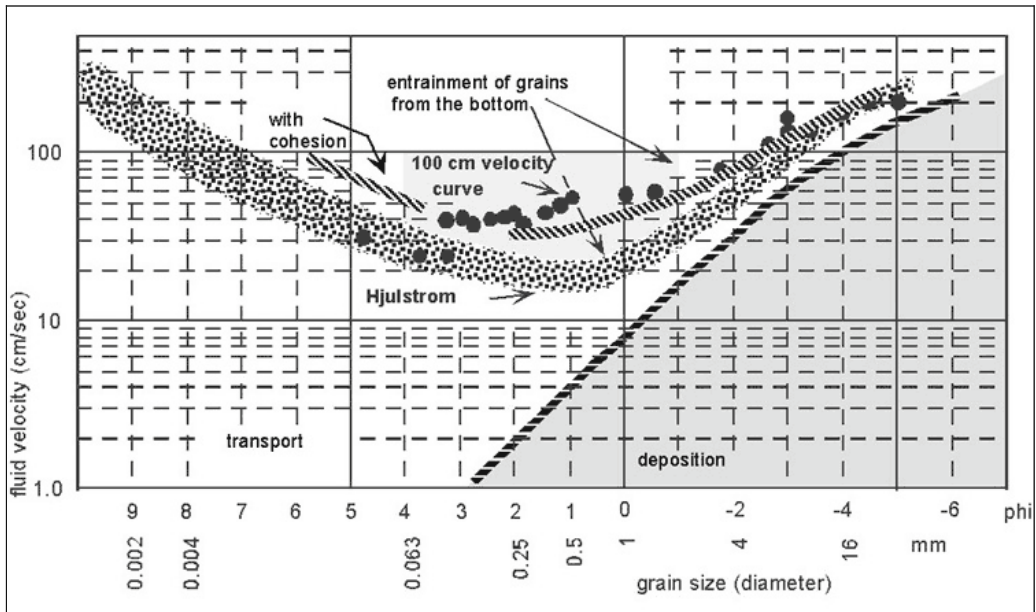
Figure 58:
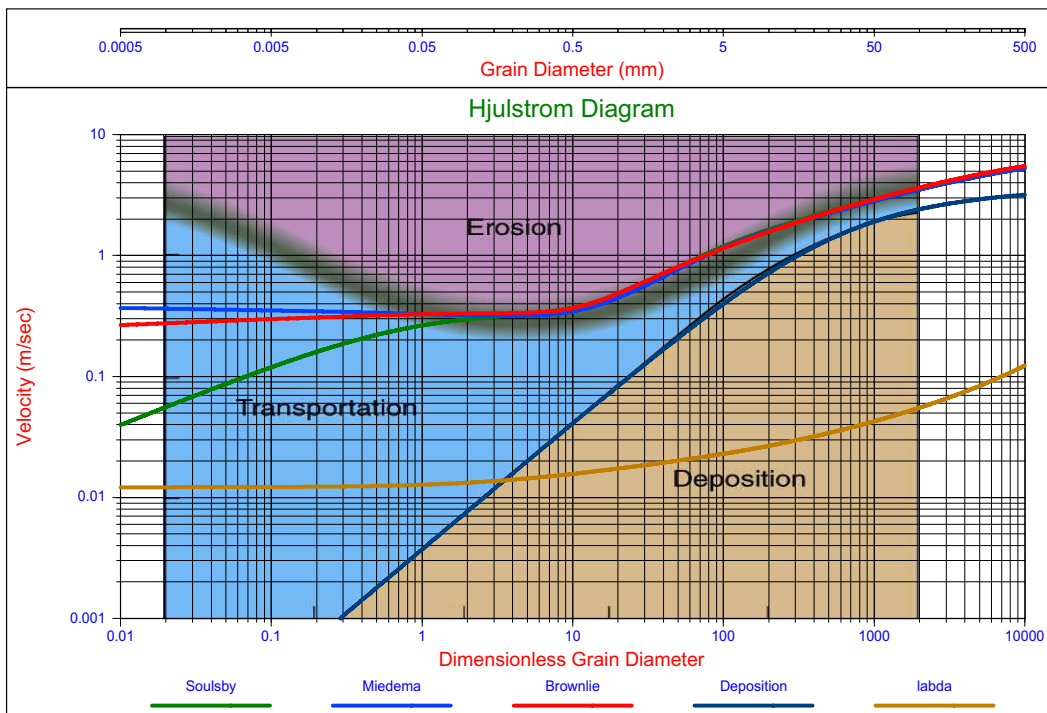
Figure 59: A comparison between the Hjulstrom curve and the Shields curve.

5.6. Friction coefficient and pressure losses with homogeneous water flow.

When clear water flows through the pipeline, the pressure loss can be determined with the well known Darcy-Weisbach equation:

$$\Delta p_w = \lambda \cdot \frac{L}{D} \cdot \tfrac{1}{2} \cdot \rho_w \cdot v^2 \tag{5.96}$$

The value of the friction factor λ depends on the Reynolds number:

$$Re = \frac{v \cdot D}{\nu} \tag{5.97}$$

For laminar flow (**Re<2320**) the value of λ can be determined according to Poiseuille:

$$\lambda = \frac{64}{Re} \tag{5.98}$$

For turbulent flow (**Re>2320**) the value of λ depends not only on the Reynolds number but also on the relative roughness of the pipe ε/D. A general implicit equation for λ is the Colebrook-White equation:

$$\lambda = \frac{1}{\left(2 \cdot \log\left(\dfrac{2.51}{Re \cdot \sqrt{\lambda}} + \dfrac{0.27 \cdot \varepsilon}{D}\right)\right)^2} \tag{5.99}$$

For very smooth pipes the value of the relative roughness ε/D is almost zero, resulting in the Prandl & von Karman equation:

$$\lambda = \frac{1}{\left(2 \cdot \log\left(\dfrac{2.51}{Re \cdot \sqrt{\lambda}}\right)\right)^2} \tag{5.100}$$

This can be approximated by:

$$\lambda = \frac{0.309}{\left(\log\left(\dfrac{Re}{7}\right)\right)^2} \tag{5.101}$$

At very high Reynolds numbers the value of **2.51/(Re·√λ)** is almost zero, resulting in the Nikuradse equation:

$$\lambda = \frac{1}{\left(2\cdot\log\left(\frac{0.27\cdot\varepsilon}{D}\right)\right)^2} \tag{5.102}$$

Because equations 21 and 22 are implicit, for smooth pipes approximation equations can be used. For a Reynolds number between 2320 and 10^5 the Blasius equation gives a good approximation:

$$\lambda = 0.3164\cdot\left(\frac{1}{Re}\right)^{0.25} \tag{5.103}$$

For a Reynolds number in the range of 10^5 to 10^8 the Nikuradse equation gives a good approximation:

$$\lambda = 0.0032 + 0.221\cdot\left(\frac{1}{Re}\right)^{0.237} \tag{5.104}$$
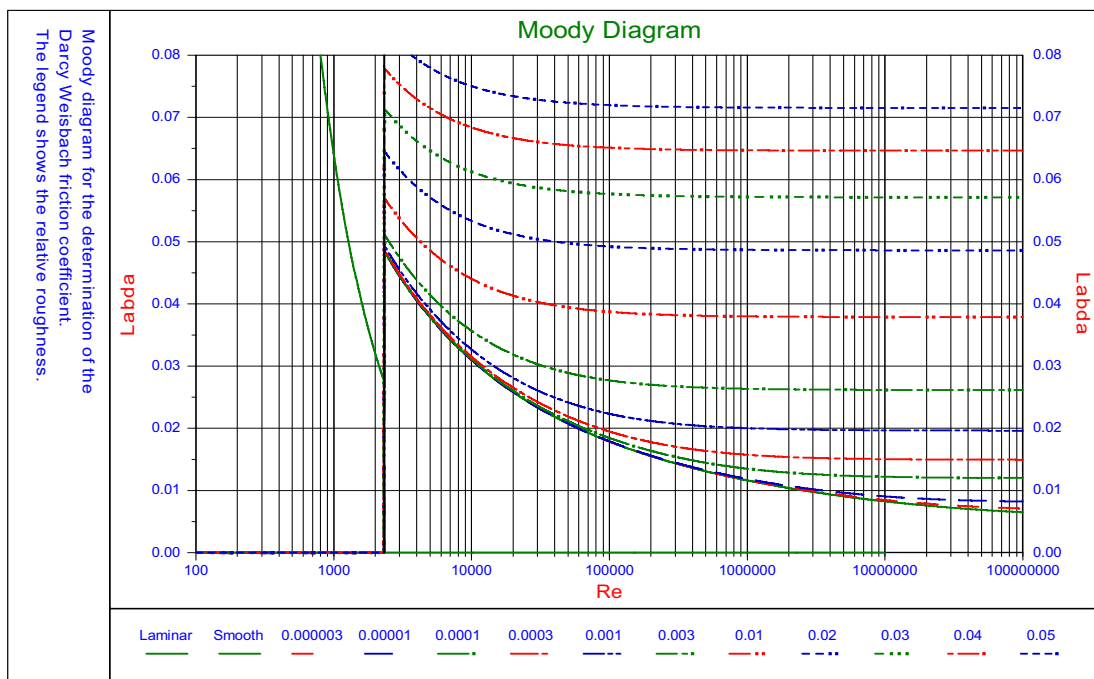
Figure 60: TheMoody diagram determined with the Swamee Jain equation.

Over the whole range of Reynolds numbers above 2320 the Swamee Jain equation gives a good approximation:

$$\lambda = \frac{1.325}{\left(\ln\left(\frac{d}{3.7\cdot D}+\frac{5.75}{Re^{0.9}}\right)\right)^2} = \frac{0.25}{\left(\log\left(\frac{d}{3.7\cdot D}+\frac{5.75}{Re^{0.9}}\right)\right)^2} \text{ Swamee Jain} \tag{5.105}$$

$$\lambda = 0.163 \cdot \left(\frac{d}{H}\right)^{0.286} \quad \text{Burt}$$

$$\lambda = 0.128 \cdot \left(\frac{k}{R}\right)^{0.333} \quad \text{Strickler}$$
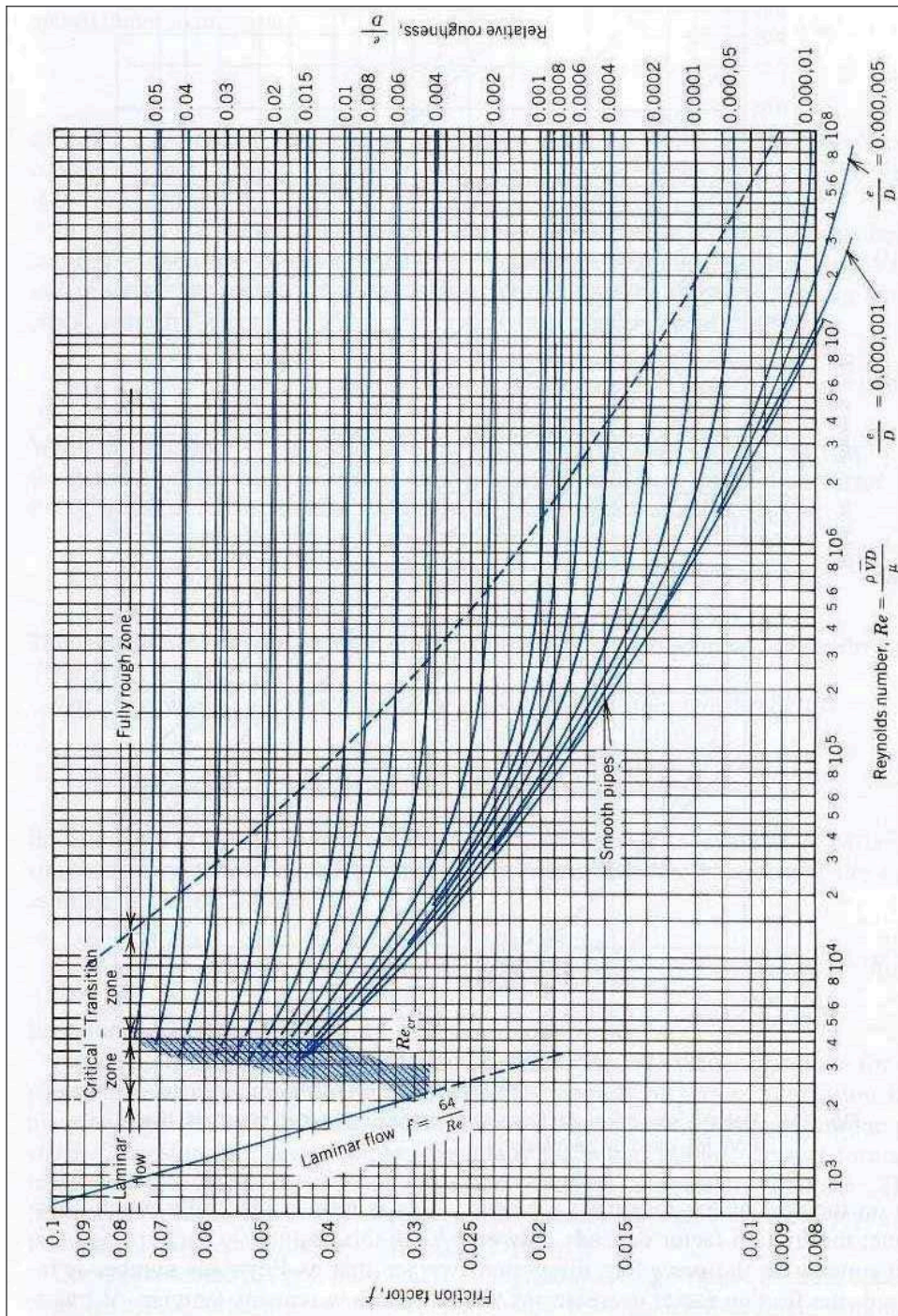
Figure 61: The original Moody diagram.

5.7. Determination of scour related to the TSHD.

After discussing the erosion phenomena extensively in the previous chapters, it is the question how to apply this in the model for determining the loading process of a TSHD. The first step is to find which particles will not settle due to scour at which average velocity above the sediment in the hopper. The relation between the shear velocity $\mathbf{u_*}$ and the average velocity above the bed is $\mathbf{U_{cr}}$:

$$\mathbf{u_*^2} = \frac{\boldsymbol{\lambda}}{\mathbf{8}} \cdot \mathbf{U_{cr}^2} \qquad (5.106)$$

Substituting this in equation 5.64 for the Shields parameter gives:

$$\boldsymbol{\theta_{cr}} = \frac{\mathbf{u_*^2}}{\mathbf{R_d \cdot g \cdot d}} = \frac{\boldsymbol{\lambda}}{\mathbf{8}} \cdot \frac{\mathbf{U_{cr}^2}}{\mathbf{R_d \cdot g \cdot d}} \qquad (5.107)$$

Re-arranging this gives an equation for the critical average velocity above the bed $\mathbf{U_{cr}}$, that will erode a grain with a diameter $\mathbf{d_s}$:

$$\mathbf{U_{cr}} = \sqrt{\frac{\mathbf{8 \cdot \boldsymbol{\theta}_{cr} \cdot R_d \cdot g \cdot d_s}}{\boldsymbol{\lambda}}} \qquad (5.108)$$

Equation 5.108 is almost identical to equation 5.55 as derived according to the simple Camp (1946) and Huisman (1995) approach. In the same way as equation 5.57 this can be written as:

$$\mathbf{d_s} = \frac{\mathbf{u_*^2}}{\mathbf{R_d \cdot g \cdot d}} = \frac{\boldsymbol{\lambda}}{\mathbf{8}} \cdot \frac{\mathbf{U_{cr}^2}}{\mathbf{R_d \cdot g \cdot \boldsymbol{\theta}_{cr}}} \qquad (5.109)$$

With a value of $\boldsymbol{\lambda}$**=0.03** and $\boldsymbol{\theta}_{cr}$**=0.05** equation 5.109 would be equal to equation 5.57.

Since the final phase of the hopper loading process is dominated by scour, the above assumption is to simple. Figure 52 shows that the grain sizes we are interested in, from 0.05mm up to 0.5mm, give Shields values $\boldsymbol{\theta}_{cr}$ of 0.2 to 0.03 if we use the original Shields curve or one of the approximation curves. The friction coefficient $\boldsymbol{\lambda}$, may vary from about 0.01 for fine grains and a smooth bed to 0.03 or higher for a hydraulic rough bed. Figure 59 shows how the value of $\boldsymbol{\lambda}$ varies as a function of the grain diameter. In the grain size range of interest this $\boldsymbol{\lambda}$ varies from about 0.01 to 0.02. This results in a range for the ratio between the Shields parameter and the friction coefficient of $\boldsymbol{\theta}_{cr}/\boldsymbol{\lambda}$ of 0.2/0.01 to 0.03/0.02, giving a range of 20 to 1.5. Equation 5.55 gives a ratio of 1.66 which is in the range and matches with grains of about 0.5 mm, giving an upper limit to the scour velocity.